Evaluation of a neural network for predicting muscle activity based on intracortical signals during gait in healthy rats

- towards restoration of locomotion of SCI using BMI

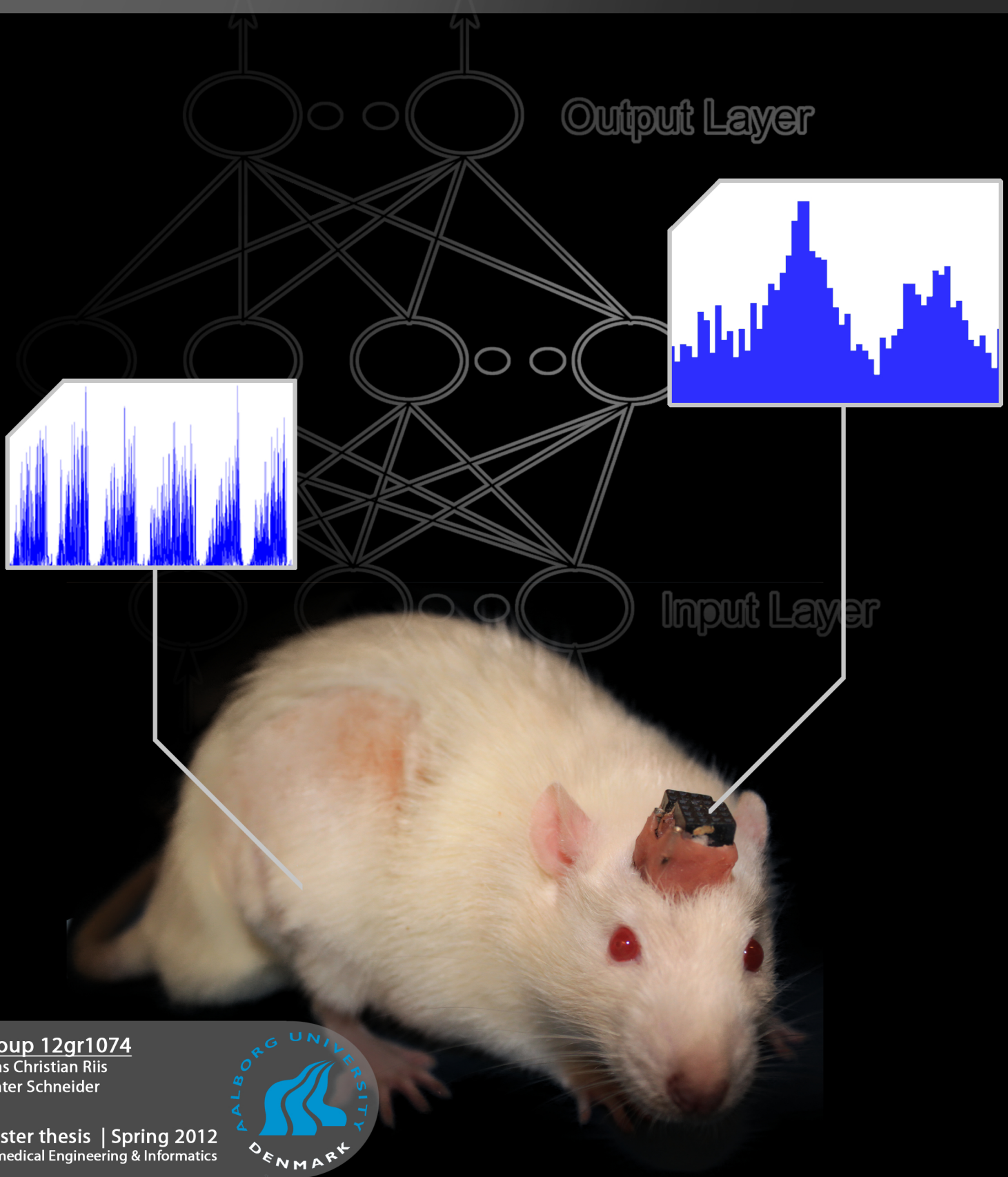

Group 12gr1074
Hans Christian Riis
Gynter Schneider

Master thesis | Spring 2012
Biomedical Engineering & Informatics

AALBORG UNIVERSITY DENMARK

AALBORG UNIVERSITY

Department of Health Science and Technology

http://www.hst.aau.dk/

Title: Evaluation of a neural network for predicting muscle activity based on intracortical signals during gait in healthy rats - towards restoration of locomotion of SCI using BMI

Theme: Applied biomedical engineering and informatics

Specialization:
Medical Systems

Project period:
22. august 2011 - 1. June 2012

Project group: 12gr1074

Group members:

Hans Christian Riis

Gynter Schneider

Supervisor:
Winnie Jensen

Editions: 4

Pages: 109

Appendices: 5

ABSTRACT:

Spinal cord injury (SCI) occur to a great extent with approximately 12.000 incidents annually in the US, inducing great expenses for carrying and treatment. SCI patients encourage restoration of gait control as one of the four most prioritized functions to regain for improving quality of life. In order to aid and restore gait control it is necessary to bridge and understand the gab between neural activity for voluntary movements and the muscle response, going around the spinal cord.

Objective of this report was to evaluate an artificial neural network (ANN) for predicting muscle activity during gait in healthy rats.

Neural activity from motor cortex (M1) and EMG signals from biceps femoris (BF) and vastus lateralis (VL) were obtained by use of 16 channel intracortical electrode arrays and intramuscular EMG electrodes in a bipolar configuration.

Four Sprague-Dawley rats were trained to walk on a treadmill with 0^o and 15^o inclination. Kinematics were calculated from high-speed camera recordings by digitizing toe, heel, knee, hip and reference markers attached on the rats. Joint angles were calculated and used to detect and extract specific gait cycles meeting the inclusion criteria.

Peri-stimulus time histograms (PSTH) were calculated for the intracortical signals and mean envelopes of maximal EMG value for BF and VL. Recordings from two rats, meeting the inclusion criteria, were used in an ANN configured on the basis of a previous study. PSTH of neural activity were used as input and envelopes of average maximal EMG value for BF and VL for output. Results from the ANN gave low R^2 values (R^2 = 0.1020) yielding an optimization problem.

A systematic optimization process of the ANN improved the R^2 value (R^2 = 0.4146) and demonstrated possibilities in predicting muscle activity by use of an ANN with neural activity from M1 as input. Further advancement and usage of prediction for control signal of FES further attention and evaluation is needed,

Findings implied future possibilities for integration in BMI applications for restoring gait control of SCI patients, if further refinement of the ANN and data are done.

Preface

This report is written by project group 12gr1074 during 3rd and 4th semester of the master education in medical systems at Aalborg University. Knowledge and practical experience have been obtained during 3rd semester in cooperation with the Miller Lab (the Miller laboratory of Limb Motor Control) at Northwestern University, Chicago and Rehabilitation Institute of Chicago (RIC). An intended outcome of pilot data did not succeed due to complications, causing new experiments to be conducted. Background, experience, ideas and complications from our stay are described in Appendix A

We would like to thank our supervisor Winnie Jensen for help, assistance and feedback during surgery and project period. Furthermore, we would like to thank Lee E. Miller, Matthew Tresch and their colleagues at the Miller laboratory of Limb Motor Control and Tresch Lab at Northwestern University, Chicago and RIC for practical experience and knowledge. A final thanks to the staff at the animal facility at Aalborg Sygehus Nord for assistance and monitoring during and after conducting surgery and animal experiments.

Reading guide

References in the report are implemented after the Harvard method, why references are indicated by [Lastname, Year]. A bibliography is to find in the back of the main report, with references ordered as they appear. Graphs, tables and listings are numbered according to its chapter, e.g the first figure in chapter 5 is numbered Figure 5.1, the second, numbered Figure 5.2 etc. The first time an abbreviation is used the word will be explained and afterwards be mentioned by abbreviation, unless full length word seems necessary.

The report is divided into 4 parts:

- Part I - Problem analysis
- Part II - Experiment
- Part III - Synthesis
- Appendicies

Contents

CHAPTER 1

Introduction

Spinal cord injury (SCI) occur to a great extent with approximately 12.000 incidents annually in the US. A total of 265.000 persons being affected by injury are estimated as of 2010. The causes of SCI are very broad (Figure 1.1), with road accidents being the primary cause of injury. The percentages have varied throughout the past years and especially violence and sports accidents have been reduced, whereas falls are raising. [McDonald and Sadowsky, 2002; NSCISC, 2011]

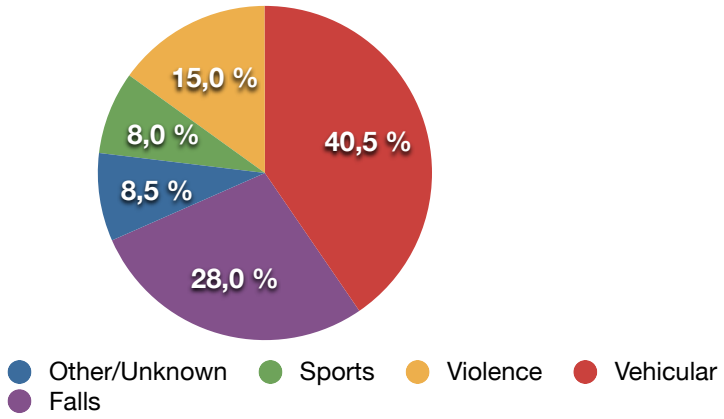

Figure 1.1: *Causes of SCI as of 2005. Redrawn after [NSCISC, 2011].*

Expenses associated with SCI varies dependent on location and extend of injury, but an estimate in the US state expenses between $500.000 and $2.000.000 as average treatment of an individual, whereas costs associated with carrying and treatment of individual spinal cord injured surpasses $8 billions annually. [McDonald and Sadowsky, 2002; NSCISC, 2011]

SCI is classified as being complete or incomplete, stating none or some neurological functions are preserved below the point of injury, respectively. Further classification and subdivision of injury depend on the individual case and level of function preserved. Functions affected by location of injury can roughly be subdivided into a cervical- (respiration, hear rate and head movement), thoracic- (posture and stability), lumbar- (gait) and sacral division (sexual function, bowel and bladder control) (Figure 1.2). [Liverman et al., 2005]

A survey covering priorities of regaining function in regard to improved quality of life (QOL) for quadriplegics and paraplegics revealed a wish for arm/-hand function (quadriplegics) and sexual function (paraplegics) having highest priorities. Following priorities were bladder/bowel control, trunk stability and walking movement. [Anderson, 2004]

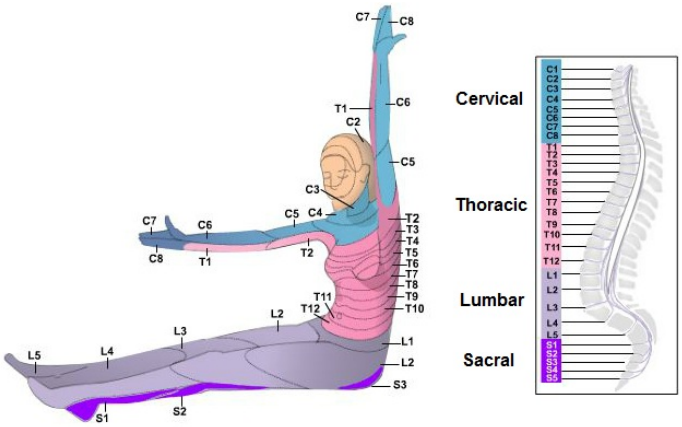

Figure 1.2: *Body regions affected by SCI, dependent on point of injury. Redrawn from [Byrne and Dafny, 2000].*

Today's research is therefore aimed towards hand function, stabilizing seated posture, gait, bladder/bowel control and sensation [Tate et al., 2011]. Commercial neuroprostheses products relying on functional electrical stimulation (FES) exist for grasping, and it is possible to restore or aid breathing, bladder control and hand function in SCI patients at the moment [Donaldson et al., 1997; Johnston et al., 2005; Keith et al., 1989; Popovic et al., 2002; Tate et al., 2011].

FES is one of todays main applied technologies in pursuing movement restoration after SCI and a potential solution [Tate et al., 2011]. FES make use of electrical bursts defined by a control signal, to stimulate e.g. motor neurons [Popovic et al., 2002]. Electrical stimulation of muscles have been known since Luigi Galvani demonstrated existence of bioelectricity [Webster, 2006].

A disadvantage of todays solutions is the limitations of control and the control signal not being enough to convey the intentions of the patient. Control signals for FES are often pre-programmed patterns for a specific movement and does not take the users intensions into consideration when eliciting an electrical burst to target muscles. [Bauman et al., 2011; Popovic et al., 2002]

An important fact is that motor commands, for carrying out voluntary movements, are independent of a SCI and still generated in the primary motor cortex (M1), but unable to reach the muscles. Decoding models are widely used in the research area of rehabilitation and seeks to fill the gab between intended movement and actual control signals for movement fed to FES. [Fitzsimmons et al., 2009; Pohlmeyer et al., 2009; Sanchez and Principe, 2007] An approach for achieving an individual decoding model is to predict muscle activity related to brain activity. A decoding model aim to decode and understand the correlation between input and output, which allow bypassing damaged tissue and thereby rebuild the lost connection from brain to muscles. [Sanchez and Principe, 2007]

Brain activity and insight in electrophysiology can be recorded and obtained in various ways with invasive or non-invasive methods like epidural-, subdural-, intracortical recordings or EEG. Epidural- and subdural recordings will give a high resolution, while the latter can monitor single unit neurons. [Wolpaw et al.,

2002] Intracortical recordings are favorable in terms of getting very specific neural activity.

Restoration of hand control, aid of breathing and bladder control have been accomplished to a great extent, whereas restoration of gait control using intracortical recordings seems very limited in the research field of biomedical engineering. [Fitzsimmons et al., 2009; Song et al., 2009]

Assessing intracortical (IC) signals from SCI patients for a decoding model imply ethical limitations. Argumentation and discussions by Gill et al. [1989] and Cenci et al. [2002] seeks to justify the use of rats as an experimental model, emphasizing similarities in motor patterns and neuroanatomy. Additional advantages of in-expenses compared with other laboratory animals and decent size for handling. Mapping of the rat brain has been done in great details and motor centers and underlying structures controlling gait have been located with high accuracy [Leergaard et al., 2004]. Bearing these factors in mind, rats seems adequate in an experimental setups a human model for assessing gait.

A schematic overview of a decoding model feeding IC signals and translating these into stimulation patterns for specific muscles coupled with gait control, could be an opportunity to bypass a transected spinal cord (Figure 1.3).

Several animal experiments have shown the possibilities of decoding intracortical or epidural signals and restoring simple hand movements, Wessberg et al. [2000] demonstrated R^2 values as high as 0.5 between actual and predicted hand movement. [Fagg et al., 2007; Slutzky et al., 2011; Wessberg et al., 2000].

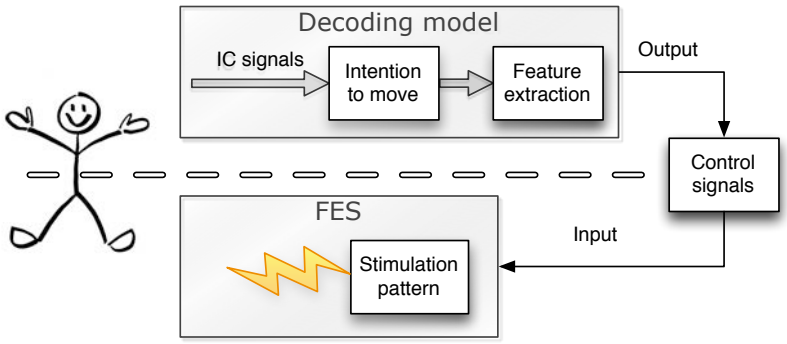

Figure 1.3: *A schematic overview of a decoding model where the output from the model is fed to the FES. IC signals are used to predict the actual intended muscle output, allowing independent stimulation instead of pre-programmed control patterns used in traditional FES.*

1.1 Initial problem formulation

To examine the correlation between brain signals planning and executing movement from primary motor cortex (M1) and muscle activity in relation to gait and use of FES.

PART

Problem analysis

CHAPTER 2

Spinal cord injury

SCI affects the nervous systems and can lead to loss of reflexes, sensation and the ability to control muscles and thereby movement.

SCI can be classified with The American Spinal Injury Association(ASIA) International Standards for Neurological Classification which are divided into four different methods that hold information about: 1) the sensory and motor level, 2) the completeness of the injury, 3) the ASIA Impairment Scale, 4) the zone of partial preservation, have maintained some motor- and sensory function above and below in complete injury cases. [Liverman et al., 2005]

The sensory- and motor level (1) is defined by the location on the spinal cord where sensory and motor functionality is intact. This is determined be touching and evaluating motor function. The completeness of injury (2) can either be complete or incomplete SCI. Complete SCI affects the patient from point of injury and functions below this point, whereas incomplete SCI still have sensory and motor functionality available below the point of injury. The ASIA Impairment Scale (3) have five different levels. Level A categorize the complete SCI, level B-D categorize three different types of incomplete SCI, and level E categorize no impairment of the spinal cord. The zone of partial preservation (4) define if the patient still have sensory or motor function after complete SCI above S5 or below the point of injury.[Liverman et al., 2005]

2.1 Loss of function

Functionality of the patients are affected accordingly to the point of injury (Figure 2.1). The loss of function affect the person from the point of injury and below at complete SCI, and in incomplete SCI the functions below the point of injury can still be functional. If the injury occur at cervical level the patient will become tetraplegic and head, neck, diaphragm and arms will be affected. If the site of injury is beneath the cervical level the patient will become paraplegic. Injury at the thoracic level affects the chest and abdominal muscles, whereas injury within the lumbar level affects the hips, legs and injury at sacral level affects the bowel, bladder, groin, calves, buttocks and legs. [Liverman et al., 2005]

2.2 Quality of life

QOL for SCI patients can change radically after injury, due to chronic pain and loss of functions. Around 60%-80% of SCI patients have chronic pain after their injury, and losing their independent lives due to loss of functions causes depression and increased suicide rates. The loss of sexual function, dysfunction of the

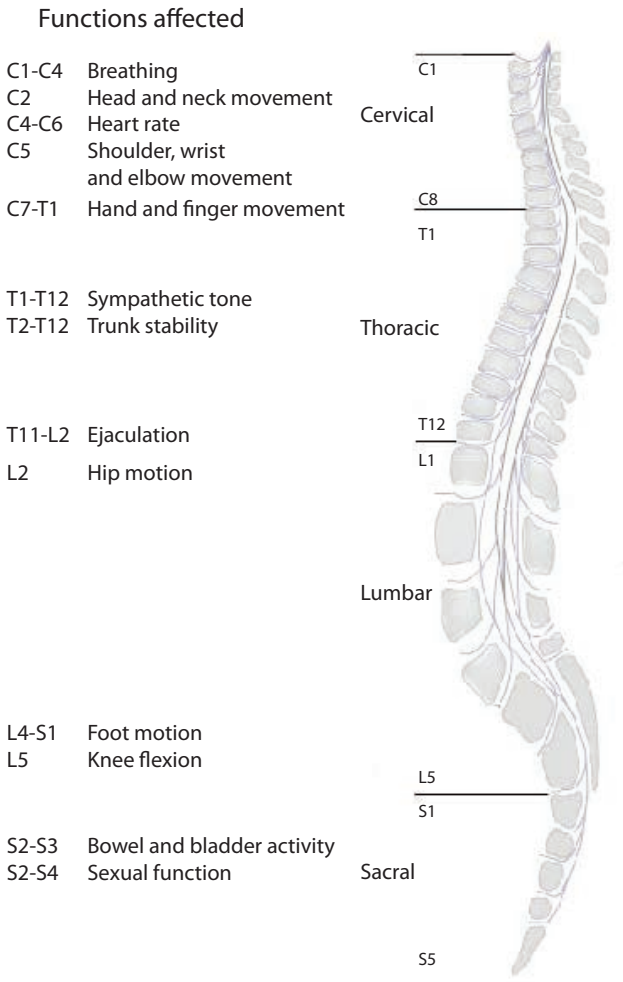

Figure 2.1: *The figure illustrate the different spinal levels and the functions affected within each level. Redrawn from [Byrne and Dafny, 2000]*

bladder and disorders of the bowel function also affects the patients quality of life. [Liverman et al., 2005]

2.2.1 Restoring important functions

In a survey published in the Journal of Neurotrauma 681 SCI Americans answered a questionnaire about recovery priorities in QOL for spinal cord injured, it was shown that regaining hand- and arm functionality was the highest priority for improving QOL for 48.7% of the tetraplegics, due to increased independence. Regaining of other functions to improve QOL as the most important for tetraplegics and paraplegics are ranked in table 2.1. [Anderson, 2004] The rankings show that both tetraplegics and paraplegics have the same priorities of regaining functions which are sexual function, increase trunk strength and balance, improving bladder/bowel function and walking function but indicated with different priority percentages.

	Regained function	Improvement of QOL
Tetraplegics		
	Sexual function	13%
	Increase trunk strength and balance	11.5%
	Improving bladder/bowel function	8.9%
	Walking movement	7.8%
Paraplegics		
	Sexual function	26.7%
	Improving bladder/bowel function	18%
	Increase trunk strength and balance	16.5%
	Walking movement	15.9%

Table 2.1: *The table show regaining of functions and improving of quality of life for tetraplegics and paraplegics [Anderson, 2004]*

CHAPTER 3

Restoring gait control with FES

Restoration of motor control is critical in order to improve QOL for SCI patients. Several options exists with the purpose of assisting or restoring motor control. Either by physical training, rehabilitation techniques or neuroprostheses. [Liverman et al., 2005]

The latter is an important discipline in biomedical engineering for pursuing restoration of motor control. FES is one of todays main applied technologies in pursuing motor restoration after SCI and a potential solution. [Tate et al., 2011]

3.1 Functional electrical stimulation

FES aim to help assisting patients accomplish voluntary movements and are widely used for restoring motor control after SCI. The conceptual idea of FES is to fetch inputs from either sensory signals or voluntary movements from active muscles above point of injury. Inputs are then sent to a controller, triggering and releasing bursts of electrical pulses to intact motor neurons. A movement can then be evoked by stimulating several nerve fibers, evoking muscle contractions in a desired pattern to carry out movement.[Liverman et al., 2005; Peckham and Knutson, 2005]

The stimulation paradigm of FES include the three parameters pulse frequency, amplitude and duration. Composition of stimulation intensity and pattern are vital in order to avoid muscle fatigue. [Peckham and Knutson, 2005]

Several electrodes exists and is chosen depending on the given application, distinguishing between surface-, percutaneous- and implanted intramuscular electrodes (Figure 3.1). Surface electrodes are noninvasive and simple to use but inadequate for stimulating deeper muscle structures or isolated areas. The percutaneous setup include an intramuscular electrode and a reference on the skin, being able to stimulate deeper structures and isolated areas inaccessible by surface electrodes. An implanted solution is used for long-term FES systems, where the electrode wires are placed under the skin and connected to an implanted stimulation controller, normally implanted in the abdomen or chest. [Peckham and Knutson, 2005]

3.1.1 Restoring gait control

Various FES approaches for restoring gait function in paraplegics have been tested. Restoring gait is a complex task which needs an interplay between factors such as balance, body posture and coordination of lower limb movements.

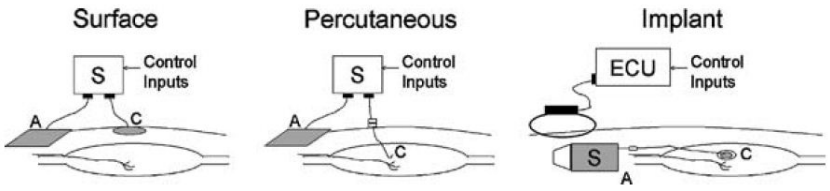

Figure 3.1: *Three different electrode setups: surface, percutaneous and implant for a FES application. S: stimulator, A: Reference electrode, C: Active electrode, ECU: External control unit.[Peckham and Knutson, 2005]*

An early approach involved stimulation of the peroneal nerve and quadriceps muscle. A reflex of the hip, knee and ankle initiated the swing phase and knee extension stance, as a response to the stimulation. This principle is incorporated in the Parastep® system, making walking over limited distances possible for paraplegics with a walker. Parastep® utilize a stimulator located on the waist, a controller in the handle of the walker and surface electrodes, allowing control of the FES system. [Peckham and Knutson, 2005]

FES systems using percutaneous or implanted electrodes for stimulating muscles of the legs have been tried. A hand operated switch was used to stimulate 48 muscles of the lower limb through a programmable microprocessor-based external stimulator (Figure 3.2). The outcome was patients being able to walk with a rolling walker as support for 300 m at a speed of 0.5 m/s. Some patients even managed to climb stairs but both scenarios required continuous training. [Popovic and Sinkjær, 2003]

Using an external branching such as the reciprocating gait orthosis is another application of FES. The orthosis support the body weight and reduce the amount of energy lost by solely using FES. This setup was not always cosmetically accepted and was very time consuming in regards to mounting. [Popovic and Sinkjær, 2003]

A newer FES experiment for SCI patients utilized implanted intramuscular electrodes in the legs, being controlled by a hand controller. Positive results were acquired and subjects were able to walk for a maximum of 1000 m at a speed of 1.1 m/s. Additionally, patients were able to stand, climb stairs and walk backwards with the given FES system. [Popovic and Sinkjær, 2003]

Research and usage of FES applications have shown a major need for physical efforts of SCI patients in order to walk. An estimation of four to six folded effort has been estimated compared with healthy persons. [Liverman et al., 2005; Popovic and Sinkjær, 2003]

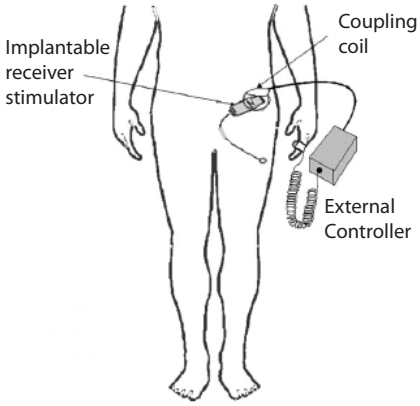

Figure 3.2: *A FES system for stimulation of the lower limb which contain an implanted receiver stimulator, stimulator electrode, a external controller, and a coupling coil which transmit information and power to the receiver stimulator. Modified from Peckham and Knutson [2005]*

A disadvantage of todays solutions is the limitations of control and the control signal not being enough to convey the intentions of the patient. Control signals for FES are often pre-programmed patterns for a specific movement, and does not take the users intensions into consideration when eliciting an electrical burst with the consequence of muscle fatigue and limited degree of freedom. [Bauman et al., 2011; Popovic et al., 2002]

CHAPTER 4

Brain Machine Interface

Moving beyond the limitations of FES and neuroprotheses to improve prospective benefits of gait restoration would require another approach. An interesting field is brain machine interface (BMI) applications, which seek to fill the gab between the brain and target device in e.g. a transected spinal cord. Research and applications aimed towards restoration of gait seems limited, so leaning against results from restoration of hand function is necessary.

Brain signals are commonly used as the starting point for BMI applications and sensory-, cognitive- or motor signals are used as input. The aim of BMI applications is to understand and decode the information given by neural activity and successfully correlate it with a given response. Bridging the gab and understanding the interplay allows the BMI to operate as the communication pathway, substituting the spinal cord (Figure 4.1). [Sanchez and Principe, 2007]

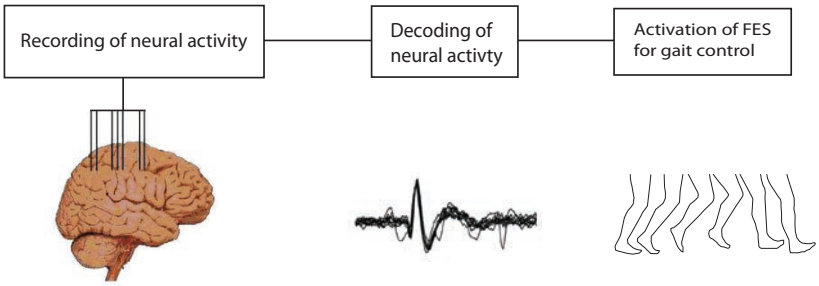

Figure 4.1: *Overview of BMI application which contain recording and processing of brain activity that can activate FES or a prosthetic. Modified from [Sanchez and Principe, 2007]*

Brain activity and insight in electrophysiology can be recorded and obtained in various ways with invasive or non-invasive methods like epidural-, subdural- , IC recording or EEG. IC recordings is a commonly used technique, since activity of single neurons can be recorded. [Wolpaw et al., 2002]

IC recordings often deploy the use of microelectrodes inserted into motor cortex, commonly in animal research. Adaption of the system interface is unnecessary when using IC recordings for BMI, being an advantage compared with other applications needing training and adaption. A disadvantage of IC recordings is the reliability of electrode performance over time. Chronical implanted electrodes can not be removed and needs to be reliable for a long time. Cell death and thereby changes in neural activity is another factor that must be taken into ac-

count when designing BMI applications to ensure stable recordings. [Sanchez and Principe, 2007]

The signal-to-noise ratio (SNR) of IC recordings is good, which allow recordings of local field potential over a brain region, multi-neuron activity and single neuron activity. Information from single- or multi neurons give knowledge about how motor neurons encode limb movements and provide important help in regard to BMI applications. [Oby et al., 2010; Sanchez and Principe, 2007]

4.1 Restoring gait control

Several methods for activating FES exists by processing neural activity. Decoding is a processing methods for BMI applications, where neural activity are used to predict a given muscle activation. The predicted signal can be fed to a FES application as control signal, stimulating the target muscles, according to neural activity.

One of the first studies evaluating restoration of gait control was conducted by Fitzsimmons et al. [2009], who also emphasized the lack of knowledge and limited documentation about the area. Restoring upper limb functionality have been investigated thoroughly and demonstrated feasibility of using IC recordings for BMI applications to control hand function. [Fitzsimmons et al., 2009]

The study by Fitzsimmons et al. [2009] evaluated the use of BMI as means of restoring gait after neurological injuries or SCI. BMI inputs consisted of neural activity recorded from M1 and S1, which were used to predict kinematics of bipedal walking (backwards and forwards) in monkeys. EMG were recorded from soleus, rectus femoris, and tibialis anterior. By use of a linear decoding algorithm the group was able to predict forward walking patterns of EMG (SNR 1.55 ± 0.39). Additional prediction of hip, knee and ankle location by XY coordinates resulted in R values ranging from 0.42 to 0.87. Remarkably higher peak rates per unit was observed during swing phase 261 ± 29 peaks/s compared to stance 87.2 ± 18.6 peaks/s. Findings suggested feasibility of cortical BMI as a rehabilitation method for gait, if the brain areas encoding gait are intact. Outputs could potentially be fed to a FES system targeting the implanted muscles, and prospectively increase QOL for patients. [Fitzsimmons et al., 2009]

A later study by Song et al. [2009] evaluated a BMI application decoding kinematics for hindlimb/trunk using rats. Neural activity was recorded from M1 using tetrodes of 24 channels in total. Kinematics were obtained by video recordings of the rats while performing gait on a treadmill. Prediction of ankle-, knee- and hip angles were done by a linear decoding model using neural activity as input. Predictions of angles at the proximal joints gave R^2 values of 0.47 ($\pm$5.0), 0.39 ($\pm$7.3) and 0.33 ($\pm$6.6) from the hip-, knee- and ankle angles, respectively. [Song et al., 2009]

4.2 Restoring of hand control

Restoration of upper limbs and grasp function have been the top priority for regaining QOL (subsection 2.2.1) and thereby also a well studied area. [Ethier et al., 2012; Fitzsimmons et al., 2009; Hochberg et al., 2006; Song et al., 2009; Wessberg et al., 2000]

Examples include a study by Hochberg et al. [2006] where hand movement was predicted, controlling a multi-jointed hand prosthetic for grasping tasks. IC signals was recorded from M1 in a tetraplegic patient, which reveled similar firing patterns with monkeys. Monkey experiments have likewise shown promising results.

A study by Ethier et al. [2012] recorded IC signals from M1 in monkeys and predicted EMG activation patterns of hand movements and grasping tasks by decoding the provided information. Patterns were used as control signals for a FES application targeting arm- and hand muscles, allowing the monkey to perform hand movement and grasping tasks under temporary paralysis.

Wessberg et al. [2000] predicted 3D hand trajectories of hand movement in real time using neural activity. The study compared decoding performance between a traditionally linear model and a newer method of artificial neural networks (ANN). Results reveled prediction accuracies of R = 0.72 (0.47 to 0.79) and 0.66 (0.42 to 0.71) for the linear model and ANN, respectively. [Wessberg et al., 2000]

4.3 Decoding of neural activity

Understanding and decoding the relationship between brain and effectuaters are necessary, in order to act as a communication pathway between brain and target muscles.

Restoration of gait require a so-called input-output mapping between neural activity and muscle activity. This I/O mapping is defined as a black box model relying on linear or non-linear solutions. Whether the input-output relation between neural- and muscle activity is linear or not is uncertain, so looking beyond linear models might be beneficial for restoration of gait.

The strength of ANN lie in the ability to model a complex nonlinear relationship. Furthermore, implementing and configuration can be done by users of minimal prior knowledge. [Tu, 1996]

Performance wise an ANN rely on configurations such as network size, learning rates and criteria for stopping to avoid over fitting. [Sanchez and Principe, 2007]

ANN have, compared with linear models, shown acceptable performance in I/O mapping studies by Wessberg et al. [2000] and significantly better in prediction of certain problems [Tu, 1996]. Further investigation of these will be conducted and background information are found in Appendix B.

CHAPTER 5

Neurophysiology of gait control

To restore and repair gait control in SCI patients it is necessary to understand how muscles work and interact with the nervous system in order to generate movement. Gait and voluntary movements have a tight interplay between the nervous system, the corticospinal pathway and the skeletal muscles [Martini, 2006].

Movements of the human body are carried out through contractions of the striated muscles in simple or complex patterns managed by the brain and spinal cord. Inputs at different levels exist and dealing with lower- and upper motor neurons. The system managing gait control is operating at different levels and can be divided into three different levels consisting of the brain, spinal cord and peripherals (Figure 5.1). Information are sent through a hierarchical structure of upper motor neurons (UMN - α motor neurons) and lower motor neurons (LMN). [Michael-Titus et al., 2010; Purves et al., 2004]

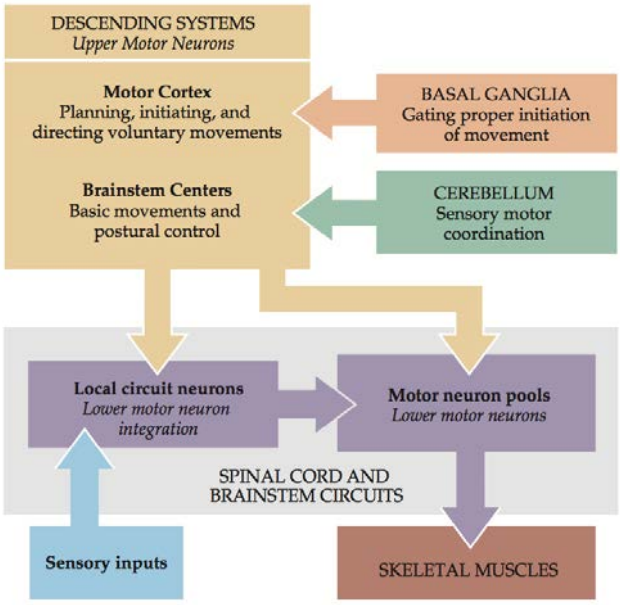

Figure 5.1: *An overview of the four subsystems composing the structure for gait control. Basal ganglia, cerebellum, descending systems and local spinal cord and brainstem circuits constitute the structure. [Purves et al., 2004]*

5.1 Gait control at peripheral level

Muscles, effectuators, are the last part of the chain from intention and initializing of gait to actually carrying out movement of the legs. The information sent to the muscles are transmitted through LMN's originating from the spinal cord and brainstem and modulate or coordinate the innervated target muscles. Movement of the legs might require fine or gross movements, which demands different accuracy. Obtaining this accuracy require the possibility to control how many muscle fibers to be stimulated. The total contraction of a muscle is expressed by the sum of tension generated in the individual muscle fibers. LMN's control a wide amount of muscle fibers, ranging from a few and up to a thousands and are innervating the striated muscles and control movements by being the last part in the command chain. This constitution of LMN's and related muscle fibers make up a motor unit. Motor units innervating a low amount of fibers are able to generate fine movement whereas a high innervation of muscle fibers assist in rough movements such as movement of the lower limb. [Everett and Kell, 2010; Martini, 2006; Purves et al., 2004]

5.2 Gait control at spinal cord and brain stem level

Local circuits of neurons in the spinal cord and brainstem control and feed the appropriate information to the LMN's. The appropriate information are fetched from within the UMN's in the brainstem and motor cortex or adjusted by sensory inputs. Sensory inputs are used to modulate or coordinate the information sent to the muscles if unforeseeable obstacles or other things require altering of the gait pattern. [Purves et al., 2004]

Previous studies have shown that sensory inputs can affect and adjust the stepping patterns when altering are necessary because of changed demands due to obstacles or bumpy ground. Inputs might descend from somatosensory input, input from vestibular apparatus or visual input. [Kandel et al., 2000]

A distinction between propriocepters and exterocepters are made in somatosensory inputs. Propriocepters are found in joints and muscles, affected by movement, whereas exterocepters remain in the skin, affected by external stimuli from surroundings and affecting the central pattern generators. This theory is supported by experiments with stepping speed of spinal and decebrated cats on a treadmill, indicating adjustments are made to match the speed of treadmill. Additional studies with cats have lead to insight of golgi tendon organs and muscle spindles regulating stepping, specifically postponing of swing phase and increasing burst activity in extensor motor neurons when transitioning from stance to swing. [Kandel et al., 2000]

5.3 Gait control at brain level

At brain level gait control is planned and initiated before effectuators in terms of muscles are carrying out the voluntary movement. Information are sent through UMN's, regulating LMN's. Axons of the UMN's form the corticospinal pathway (pyramidal- and extrapyramidal tract) arising from motor cortex and the brain stem. Initiating movements and ensure correct posture are some of the important functions of the corticospinal pathway. [Purves et al., 2004]

Higher level inputs from the basal ganglia and cerebellum regulate the local circuits and LMN's through modulation of UMN's and ensure spatial and temporal precision of movements, since the basal ganglia and cerebellum does not have any direct connection to the LMN's. [Martini, 2006; Michael-Titus et al., 2010; Purves et al., 2004]

Neural recordings from areas at brain level have shown rhythmically patterns during locomotion, indicating a participation in the more general motor pattern. Visual input fed to the motor cortex has shown a huge influence on regulating stepping patterns where visual information are critical, like walking on ladders or other demanding tasks. [Kandel et al., 2000]

CHAPTER 6

Analysis of gait control

Locomotion, a degree of freedom and vital ability for humans and animals to move from one place to another. Daily walking is a stereotypic action, carried out without any further thoughts, being able to adapt the walking pattern to unforeseen obstacles or other sudden changes in the environment. Stereotypic and repetitive actions imply automatically adjustments in the lower levels of the nervous system, where intervention from higher level centers seems unnecessary. Studying cats and dogs have to a great extent given knowledge of walking patterns and neural mechanisms controlling movement. [Kandel et al., 2000; Roy et al., 1991]

6.1 Decomposition of locomotion

The step cycle is often divided into swing and stance to get a better understanding and examining locomotion in humans and animals. Swing (transfer) phase, when the foot is without contact to the ground, can be divided into sub-phases flexion (F) and first extension (E_1), whereas stance (support) phase, when the foot is in contact with the ground, can be divided into second extension (E_2) and third extension (E_3) - (Figure 6.1). A greater insight into the phases can be obtained with knowledge from a biomechanical point of view including kinetics, kinematics or EMG activity during locomotion. Further information can be achieved through a neurological aspect. [Kandel et al., 2000; Rossignol, 1996]

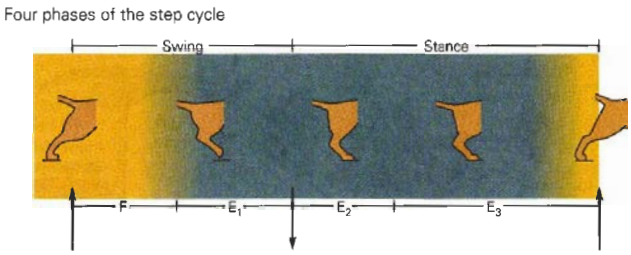

Figure 6.1: *Overview of the step cycle with swing- and stand phase divided into flexion and extensions. Arrows indicate lift-off and landing. [Kandel et al., 2000]*

From swing phase, starting at lift-off, flexion of the hip, knee and ankle is carried out and lifting the leg up under the body (F). Around halfway throughout the swing phase and beginning of E_1, the hip keeps flexing, while knee and ankle starts counter moving due to extension. Moving the lower leg ahead and preparing for ground contact is the end of swing and beginning of stance. After the

transfer phase (F to E_1) E_2 is marking the beginning of the support phase (E_2 to E_3). During the first part of stance knee and ankle are briefly flexing, while all joints are extending during E_3 shifting the body weight. Locomotion is executed smoothly due to the tightly interaction between flexors and extensors during the phases, defined as motor pattern for stepping. [Kandel et al., 2000; Rossignol, 1996]

6.2 Biomechanical point of view

Different approaches and techniques for analyzing and measuring gait exist. The common approaches are kinetics, kinematics and EMG. Kinetics describe the internal and external forces that causes movement and can be obtained through different transducers. Kinematics leave out the kinetics and focus on the geometry of movement, obtained by video recordings and subsequent digitization of coordinates. EMG examine the activation patterns of specified muscles during a repetitive task. [Back and Clayton, 2000]

Kinetics will not be elaborated since forces are outside the focus area.

6.2.1 Kinematics

When conducting kinematic analysis, the experimenters are interested in temporal, linear and angular information describing the gait. Video recording is commonly used for kinematic analysis in interplay with digitization software.

Video recording
Todays high-speed cameras make it suitable for kinematic analysis of gait in animals or humans. Studies have shown that recordings at 60 Hz is adequate for equine locomotion, whereas other studies have used 125 Hz to 200 Hz for rats [Back and Clayton, 2000; Gillis and Biewener, 2001; João et al., 2010]

The frequency should be determined in the light of event to examine. For short cycles and fast movements a higher frequency is desired to ensure that no information are lost. Lighting becomes an import factor when utilizing high-speed cameras, since fast shutter speed require better lighting conditions to ensure a sharp picture and accentuate markers attached to the skin. [Back and Clayton, 2000]

Markers
Skin markers are needed to define the line segments between points of interest. Studies of locomotion often include hindlimb markers at the toe, heel, knee and hip to quantify joint angles and temporal/linear movement of the hindlimb (Figure 6.2). [Back and Clayton, 2000; Gillis and Biewener, 2001; João et al., 2010; Kandel et al., 2000; Leblond et al., 2003; Pearson et al., 2005; Rossignol, 1996]

For auto digitizing videos, well defined markers with sufficient contrast between skin and markers are necessary. Black colored or retro reflective material markers has shown to improve the contrast together with ambient lighting of 300 W to 800 W. [Back and Clayton, 2000; Gillis and Biewener, 2001]

The experimenters should consider the repeatability and reliability of position-

ing the markers if these are removed or falling off in-between recordings. Especially at points where loose skin account for the movement, leaving the marker more or less stationary.

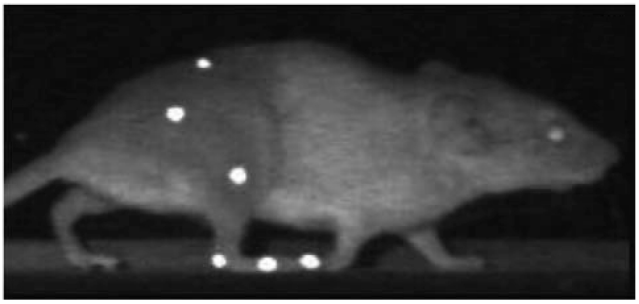

Figure 6.2: *An example of positioning markers on a mouse with retroreflective tape. [Pearson et al., 2005]*

After digitizing the points and saving the coordinates of the individual points in a two or three dimensional space, it is possible to do further calculations. Depending on the objectives of the study, temporal, linear or joint angles are know possible to calculate. Dividing the locomotion into phases as described in section 6.1 allow the calculation and defining phases by use of joint angles and video synchronization.

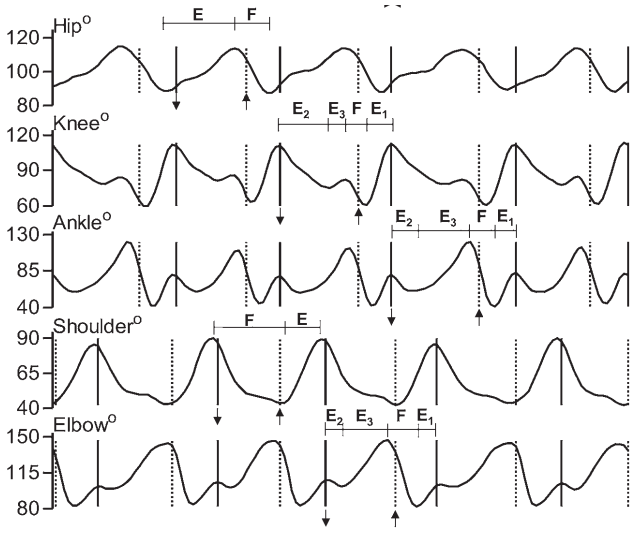

Figure 6.3: *Change in joint angles during five cycles for hip, knee, ankle, shoulder, and elbow during rat locomotion. Lift-off and toe-down is indicated with up arrow or down arrow, respectively. Sub-phases F, E_1,E_2 and E_3 are indicated. [Thota et al., 2005]*

Plotting the change in joint angles during locomotion should yield a recognizable cyclic pattern for each gait cycle (Figure 6.3).

Another common representation is by connecting the points, forming limb segments, for each video frame composing stick figures (Figure 6.4). These figures can reveal modification in locomotion or differences between two tasks by visual examination.

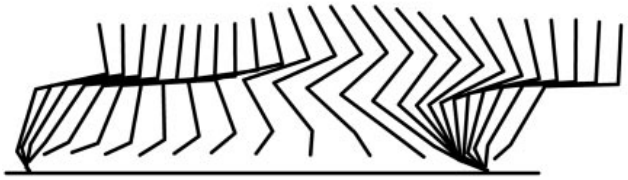

Figure 6.4: *An example of a stick figure showing the sequential positioning of forelimb movement in a rabbit during one gait cycle from lift-off to lift-off. [Beloozerova et al., 2003]*

6.2.2 EMG activity

EMG recordings are used to represent the activity of a single muscle or group of muscles. In terms of locomotion EMG recordings from the hindlimb can help describing the pattern of muscle activity. The amplitude of an EMG signal depict the electrical intensity of a muscle contraction. [Webster, 2006]

Different types of electrodes are used to record the muscle activity, chosen upon objective for the experiment. Generally EMG is separated into surface EMG (sEMG) and intramuscular EMG (iEMG) having their disadvantages and advantages. sEMG is often chosen if a general gross activity of a muscle group is decided, whereas iEMG record from individual fibers and represents the individual motor unit action potentials. [Bronzino, 1999; Webster, 2006]

In terms of locomotion, single unit information are desired to get a clear distinctive pattern between muscles but choice of subjects and tasks may limit or favour the type of EMG.

An example of raw iEMG signal obtained from hindlimb muscles of a mouse (Figure 6.5). It is clearly to identify the bursts due to contraction and the alternation between activity in left and right leg during locomotion. This clearly distinction of muscle activity pattern might not be as visible due to artifacts and noise from the surroundings.

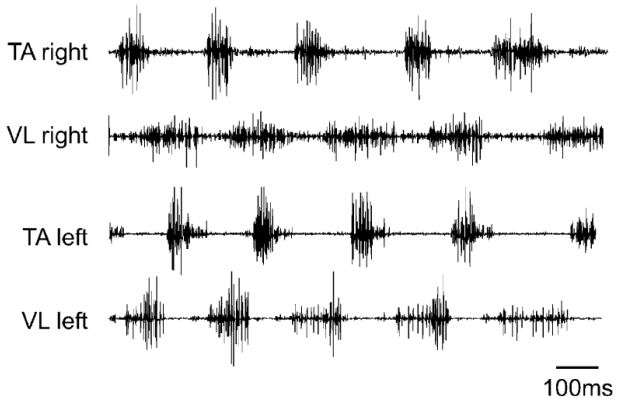

Figure 6.5: *iEMG recordings from the hindlimb muscles (Tibialis Anterior and Vastus Lateralis) in a mouse running on a treadmill. [Pearson et al., 2005]*

Therefore, post-processing of EMG signals in terms of locomotion analysis is applicable. Interesting information regarding locomotion may include recruitment level of the muscles, activation pattern of elected muscles and synchronization with kinematic results (subsection 6.2.1).

Detecting muscle activity pattern
EMG recordings from the hindlimb can help describe patterns of muscle activity during locomotion. Defining the muscle activity is often done by rectifying the raw signal and filtering with a low-pass filter or moving average filter. This action produces an envelope of the EMG signal and emphasize the phases where muscles are active or passive (Figure 6.6).

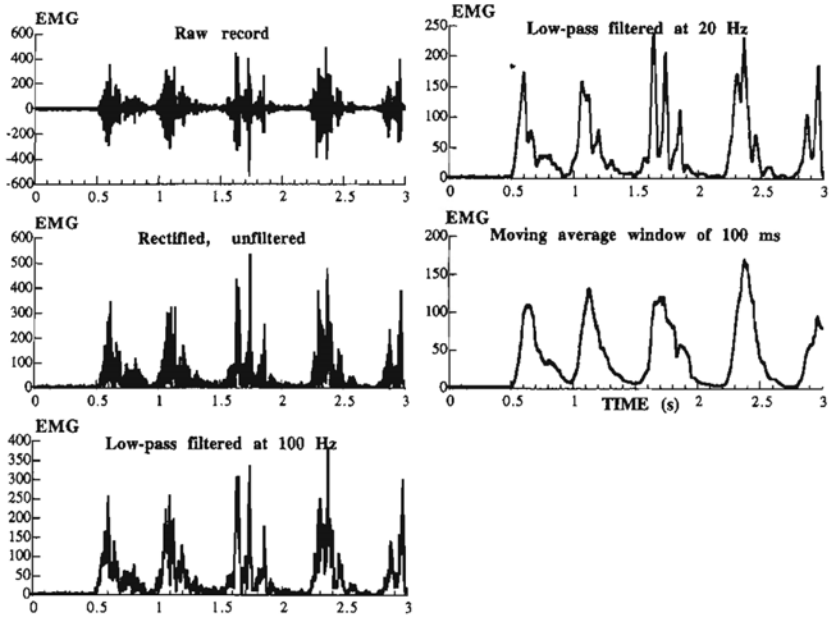

Figure 6.6: *Demonstrating the steps in retrieving the envelope of an EMG signal. Differences in the envelope is seen depending on the filtering method. [Latash, 1998]*

Calculating an envelope of the EMG signal ease the identification of the timestamp where the muscle is activated. Knowing the period of time where a muscle is activated, can be valuable information in analysis of locomotion.

Observed muscle activity might vary between recordings/subjects due to factors influencing the muscle activity. Factors like condition of the subject, physical shape, walking pattern, fatigue and type of EMG electrodes/placement may affect the results, just to mention a few, but previous studies have lead to a general overview of muscle activity in cats with a consistent repetitive pattern across experiments (Figure 6.7). [Rossignol, 1996]

Muscles of interest and implementation
A large amount of hindlimb muscles are activated during gait control (Figure 6.7). Due to the size of smaller research animals implantation of intramuscular electrodes in the lower limbs can influence the movement of the knee joint and affect the gait pattern. Implanting intramuscular electrodes in the thigh region is there-

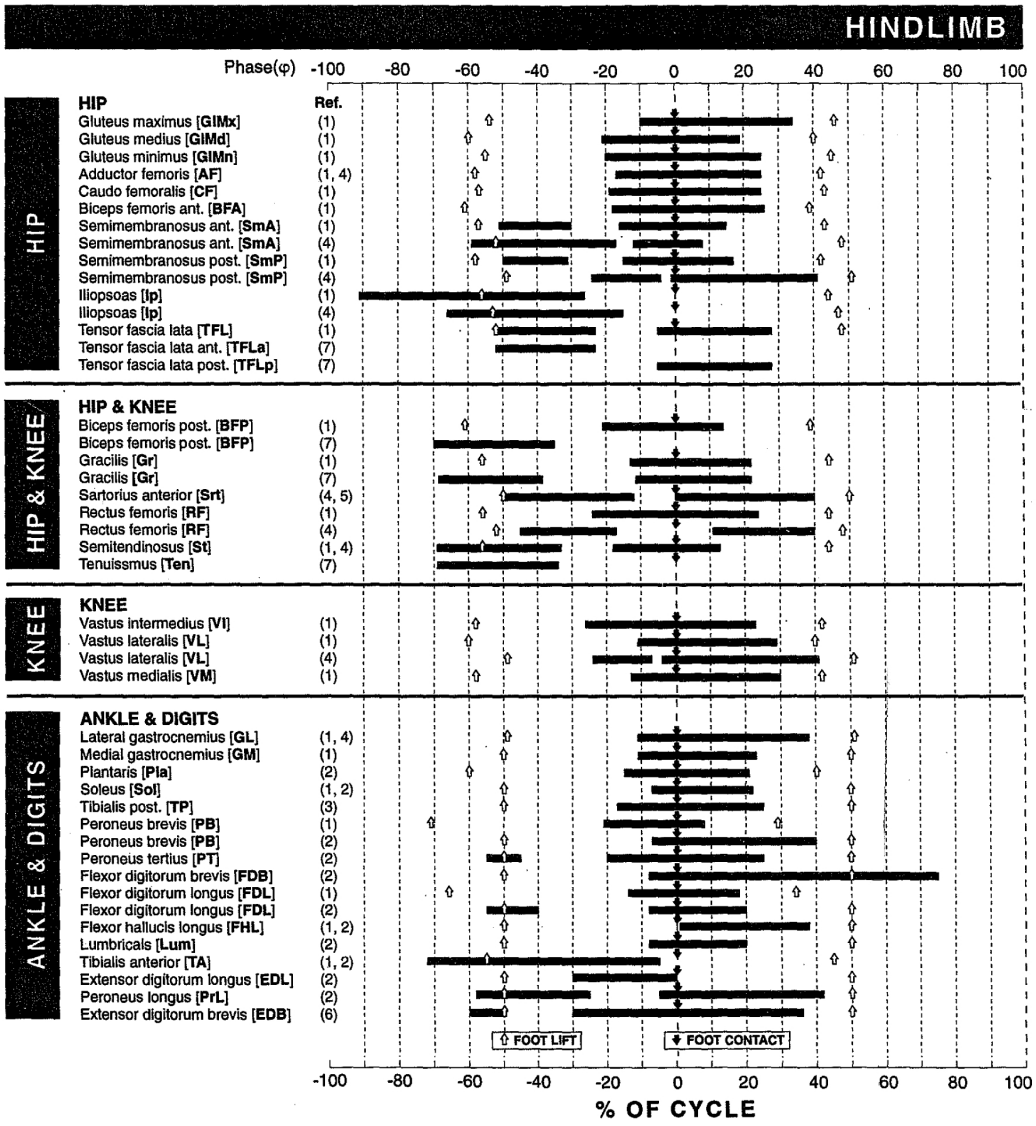

Figure 6.7: *Overview of hindlimb muscle activity from cats during trot. Toe-down is stated by downward arrows and lift-off with upward arrows. EMG patterns were obtained from different sources and synchronized around toe-down. [Rossignol, 1996]*

fore preferred to avoid mechanical stress and maintain a normal gait pattern. When implanting intramuscular electrodes in smaller animals it is beneficial to choose larger superficial muscles to ensure the electrodes will be implanted in the correct muscles and depth. [Pearson et al., 2005]

6.2.3 Linking kinematics

Combining the different kinematic information will help getting an overview or reveal characteristics/patterns in locomotion. By synchronizing joint angles, EMG and muscle activity patterns around an event (typically lift-off or toe-down) repeating patterns might appear (Figure 6.8).

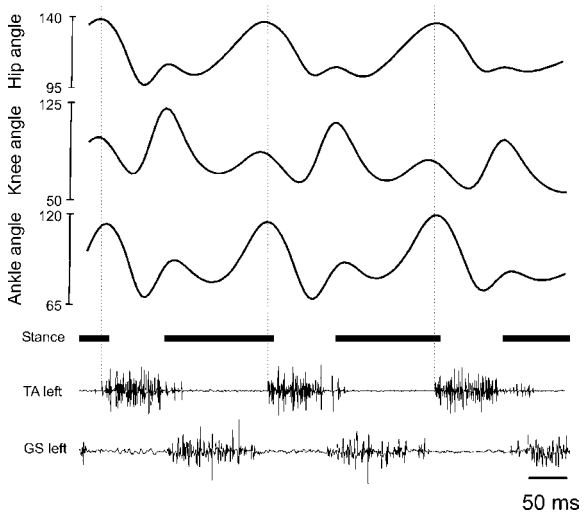

Figure 6.8: *Synchronizing joint angles, EMG and stance time with respect to activation of tibialis anterior. [Pearson et al., 2005]*

6.3 Evaluation of the treadmill for assessing gait

The treadmill is a widely used tool for assessing e.g. locomotion, neuroscience research or behavioral studies, whether it is rats or other animals [Back and Clayton, 2000; Drew, 1988; Fitzsimmons et al., 2009; Pearson et al., 2005; Pereira et al., 2006].

The force of treadmill usage lie in the control of speed and convenience of test and training, allowing evaluation of other factors in a standardized and reproducible environment [Pereira et al., 2006].

A study by Pereira et al. [2006] examined the comparability between rat locomotion on treadmill and overground and suggested comparability if adequate velocity was chosen. Duration of step cycle and stance phase on treadmill were significantly longer and overground running had a greater flexion at hip, knee and angle joint.

A theoretical constant speed on the treadmill might deviate due to frictional forces during stance phase. Especially for heavy animals, where a reduction of 9 % in speed has been observed for equine locomotion. [Back and Clayton, 2000]

CHAPTER 7

The rat as an experimental animal

Ethical rules are the limitational factor in the research field of SCI, motor function and biomedical engineering applications for humans. Since human recordings from the brain centers altering gait is not possible, a resort to rats are chosen and this chapter will justify the aspect of comparability between humans and rats as a human model. Furthermore, known and documented knowledge regarding kinematics and intracortical recordings in animals will be examined.

7.1 The rat as a human model for assessing gait

Rats and humans are at first glance different by appearance. Factors as size or gait pattern due to quadrupedalism seems evident. Rats are widely used in research areas as immunology, physiology, neuroscience and aging in spite of these visual deviations [Gill et al., 1989].

Opinions by Cenci et al. [2002]; Gill et al. [1989] seek to justify and discuss the comparability between rats and humans and the usage of rats as an experimental animal. Overall audit agrees in homology in between rats and primates through comparative studies. Motor patterns across species in rats and primates seems comparable, though differences in brain structure and neural system exists. Motor cortex and somatosensory cortex are organized differently and partly overlap each other in rats, whereas primates are clearly separated.

Neuroanatomical studies have shown functional similarities for neural systems controlling movement and organization of circuits such as basal ganglia, important for motor responses. There is no denying that rat studies are inexpensive and serve as an effective complement to primate studies, where comparability seems adequate. [Cenci et al., 2002; Gill et al., 1989]

The muscle contraction related to a gait cycle can be divided into four phases for humans and quadrupeds, these phases are flexion, first extension, second extension, and third extension(Figure 6.1) [Kandel et al., 2000]. Muscle activity from the hindlimb during gait show similarities between humans and quadrupeds, where several muscles have same activation patterns which e.g. include vastus lateralis, biceps femoris and tibialis anterior. [Vaughan et al., 1999]

Similarities in phase duration of gait exist between humans and rats. The ratio between swing- and stance phase for humans are in the range of 38% to 40% / 60% to 62% (Figure 7.1) compared with approximately 36% to 37% / 63% to 64% in rats walking at speeds lower than 48 $\frac{cm}{s}$ (Figure 7.3). [Gillis and Biewener, 2001; Vaughan et al., 1999]

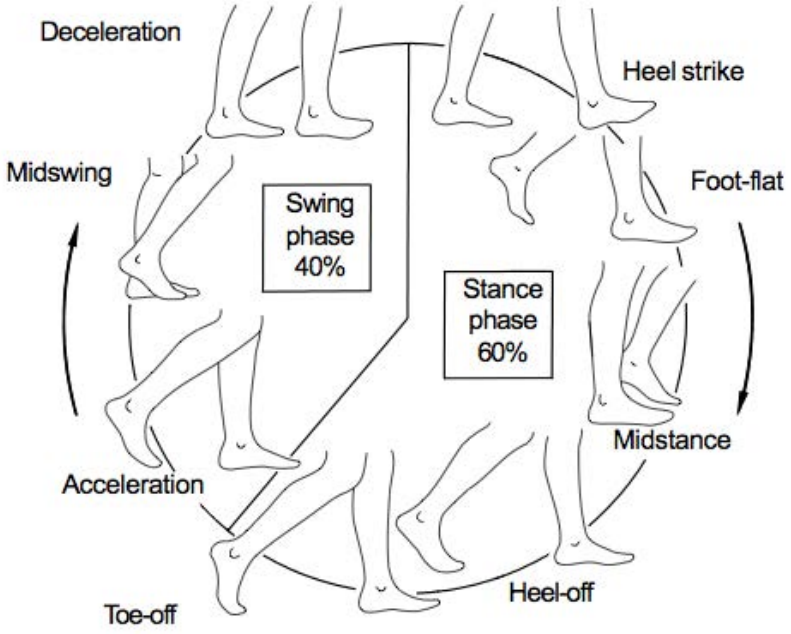

Figure 7.1: *Percent wise duration of phases in the human gait. [Vaughan et al., 1999]*

Motor- and somatosensory cortex

Similaritites within the corticospinal tract between humans and rats have been documented, although the amount of corticospinal neurons are greater in humans due to differences in brain weight and size. The corticospinal tract originate from layer V in the cerebral cortex. The majority of corticospinal neurons are located in primary motor cortex (M1) and primary somatosensory (S1) cortex for humans and rats (Figure 7.2). Corticospinal neurons originating from the ventral premotor cortex (PMv) in humans can be linked to the rostral forelimb area (RFA) in rats. Differences exist in the subdivision of M1, where a subdivision into supplementary motor area (SMA), dorsal premotor cortex (PMd), cingulate motor areas (C) and PMv is possible. Studying the rat has revealed a subdivision in only two motor areas, caudal forelimb area (CFA) and RFA. This finer subdivision is also maintained for the somatosensory areas S1 and S2, where areas in primates include 3a, 3b, 1 and 2. Subdivision of the areas (Figure 7.2), where the rat brain also reveal an overlap between M1 and S1. [Nudo, 2007]

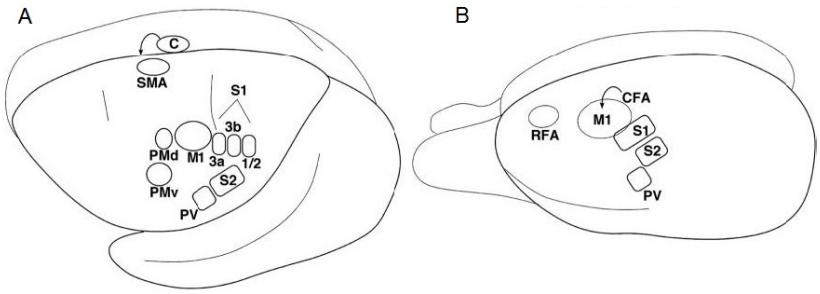

Figure 7.2: *A comparison between primates (A) and the rodents (B) reveal differences in regard to motor- and somatosensory areas. Same overall division maintain between primates and rodents but further subdivision of M1 (PMd, PMv, SMA and C) and S1 (3a, 3b, 1 and 2) is possible in primates. [Nudo, 2007]*

7.2 Previous research and findings

Previous studies have assessed kinematics, intracortical signals and EMG within rats.

Electromyography and kinematics

In Gillis and Biewener [2001] EMG and kinmatics was investigated during gait from biceps femoris and vastus lateralis, which are two of the largest muscles of the rat hindlimb. The results showed that biceps femoris and vastus lateralis were activated in bursts and overlapped each other during the stance phase, as seen in 7.3. Regarding kinematics for a gait cycle the hip angle interval was found to be 90^o at stance and 110^o at lift-off, and the knee angle interval was found to be 110^o at stance and 75^o at lift-off. Results from different gait speeds showed different muscle activation patterns for each muscle and between the two muscles at different times. Within the different gait speeds the EMG activity of biceps femoris generally activates just before the start of the stance phase and stops in the last half of stance phase. The vastus lateralis has quite the same activation pattern as biceps femoris except for a low EMG activity in the end of the swing phase. The EMG intensity for both muscles increases in regards to higher gait speeds. [Gillis and Biewener, 2001]

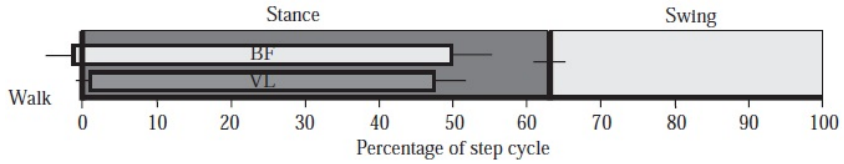

Figure 7.3: *The EMG mean activation period with standard diviation is represented from the horizontal bars from biceps femoris and vastus lateralis. The gait cycle is divided into stance and swing phase and the walking speed are 36 $\frac{cm}{s}$. [Gillis and Biewener, 2001]*

Intracortical recordings

Chapin et al. [1999] recorded IC signals from the forlimb motor cortex area in six rats. Cortical microwire electrodes were implanted from where neural motor activity were recorded when the rat pressed a lever. In the six rats activity from 21-46 single neurons were recorded during the experiment. With the recorded motor responses it was possible to predict 87% of the lever movements in all animals with simple thresholding of the neuronal population. Prediction with ANN was also performed which gave accurate results, R = 86.

In Jensen et al. [2006] IC recordings were made from the M1 in a rat. A 16 channel tungsten wire array was inserted in the forelimb area of the MI and the ulnar nerve was stimulated. When stimulating the ulnar nerve it was possible to record the corresponding motor response in M1.

CHAPTER 8

Motivation of choices

Restoring and aiding hand function through BMI and neuroprostheses have been investigated to a great extent and shown promising results. Same investigation and results are still lacking in regard to restoration of gait and conducted research are limited. Showing promising results could be crucial for spinal cord injured with lower limb paralysis and a step towards restoration or aiding gait. Benefits would not only be in terms of lowered expenses associated with SCI but also improved quality of life among the afflicted.

Success criteria for restoration of gait through BMI could be extracting information about speed, direction, position of joint angles or gait duration, but an ultimate success criteria would be to retrieve neural activity of intended movement, decode activity and generate a dynamic control signal for FES to target muscles.

In order to extract neural activity of intended movement, it is decided to do recordings from M1 because this area handle planning, initializing and directing voluntary movements. This choice imply invasive procedures not applicable for human research, so it is necessary to involve experimental animals. Rats are chosen on the basis of allowed research animals in Denmark, since they are relatively inexpensive (compared with other animals), decent in size for handling and easy to train.

Rats have proven reliability in several experiments and shown similarities with human physiology. Especially similarities in motor patterns and neuroanatomy advocate the use of rats. Furthermore, mapping of the rat brain has been done in great details and motor centers and underlying structures controlling gait have been located with high precision.

An experiment is set up where neural activity from M1 are extracted in healthy rats during normal gait at a treadmill with constant speed. The treadmill allow a well controlled environment with constant speed and opportunity of applying inclination. Recordings from M1 will be done under two behavioral tasks, while running horizontal on treadmill and running with inclination. It is believed that neural activity patterns and muscle activation regarding gait are enhance during demanding tasks.

Muscle activity will be recorded by EMG electrodes implanted in the hindlimb muscles biceps femoris (BF) and vastus lateralis (VL), being a hip and knee extensor, respectively. Choice of muscles is a tradeoff between desired muscles and invasiveness. The muscles are located in the thigh, fairly superficial and easy to access, making the operation less invasive and improve the survival rate of the rats. Muscle activity of BF and VL have been evaluated in previous studies allow-

ing the opportunity to compare results and lean against their methodology.

Kinematic analysis will be carried out in order to asses further information describing gait pattern. Neural activity will be fed to an ANN with muscle activity as target.

ANN has shown positive results in predictions based on cortical neurons and can potentially be trained to any complex input-output relations.

Sensory input and obstacles requiring alterations of gait are left out of the scope and focus will be on stereotypic and repetitive patterns of gait.

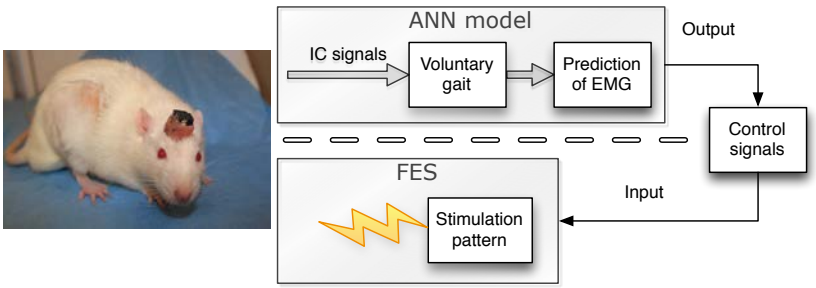

Figure 8.1: *A schematic overview of the desired ANN model for predicting EMG.*

8.1 Project hypothesis

Intracortical neural activity, extracted from M1, can predict EMG activity of the hindlimb muscles BF and VL in healthy rats with the use of ANN. The experiment seek to decode and understand correlation between neural activity and muscles for horizontal and inclined treadmill walking at constant speed, in order to predict activity by use of an ANN.

PART

Experiment

CHAPTER 9

Experimental protocol

The experiment seek to decode and understand correlation between neural activity and muscles for horizontal and inclined treadmill walking at constant speed, in order to predict activity by use of an ANN. To reach this aim neural activity from the hindlimb area of M1, iEMG signals from BF and VL and kinematics will be recorded from healthy rats during locomotive tasks on a treadmill.

The experimental protocol is based on experience from a pilot study where surgical procedures was practiced and experimental setups tested.

9.1 Equipment

The following materials were used during the experiment.

Tucker-Davies Technologies System (TDT)

- RX5 Pentusa Base Station
- RA16PA 16-channel medusa pre-amplifier for IC
- RA16CH 16-channel chronic headstage for IC
- IC electrode array with custom made adaptor
- RA4PA 4-channel medusa pre-amplifier for EMG
- RA4LI 4-channel headstage for EMG
- EMG electrodes with custom made adaptor

Camera

- High-speed camera (Basler A602fc-2)
- 2 x 400 W telescope work lamps (SARTANO)
- Black markers

Treadmill

- Treadmill including perspex cage - conveyor belt with a width of 40 cm and length of 100 cm (Letica Scientific Instruments AUC Institute 8 no. 33558)
- Mini lifting jack
- Voltmeter
- Resisters with 15 Ω and 22 Ω
- 12 V Battery (MFD. by YUASA corp. for ENERSYS inc.)

Computer

- DT340 card (PCI bus digital I/O and counter/timer board)

- Video recording and processing software Vicon Motus 9.2 (Vicon Systems, Oxford, Great Britain)
- Real-time Processor Visual Design Studio (RPvdsEx) software

Miscellaneous

- Grass stimulator (Model: SD9J, S/N: 99A0543G)
- Grass Photoelectric stimulus isolation unit (Model: PSI06, S/N: 03K01026)
- Shaver
- Tape

9.2 Experimental setup

The following part describing the experimental setup is divided into two parts, a hardware and software part, and a part describing the preparation process of the rats.

Hardware and software

The experimental setup is depicted in Figure 9.1

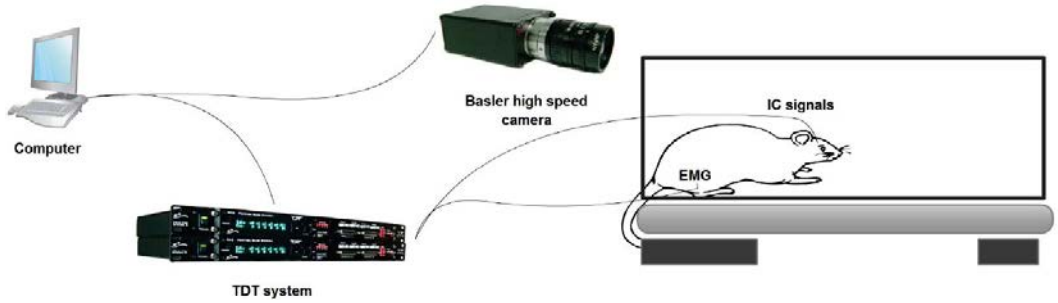

Figure 9.1: *The experimental setup of equipment for continuous recording of high-speed video, EMG and IC snippets during rat locomotion on a treadmill.*

TDT setup

A TDT system was used to record IC- and EMG signals while the rat was walking on the treadmill. Custom made IC electrode arrays was connected to a RA16PA pre-amplifier through a RA16CH headstage with a custom made adaptor. The EMG electrodes were connected to a RA4PA pre-amplifier through the RA4LI headstage with a custom made adaptor for the EMG electrodes. The pre-amplifiers were connected through fiber-optics to the RX5 Pentusa Base Station. Data were streamed to a computer equipped with a DT340 card (PCI bus digital I/O and counter/timer board) for offline processing. [TDT, 2011]

DSP	100 MHz Sharc ADSP 21161, 600 MFLOPS Peak
Memory	128 MB SDRAM (Shared)
D/A	16-bit PCM
Sample Rate	Up to 97.65625 kHz
Voltage out	+/- 10.0 V
S/N (typical)	84 dB (20 Hz to 25 KHz)
Output impedance	10 Ω

Table 9.1: *RX5 Pentusa Base Station [TDT, 2011]*

Headstage gain	20x
Highpass filter	2.2 Hz
Lowpass filter	7.5 kHz
Input impedance	10^6 Ω

Table 9.2: *RA4LI headstage [TDT, 2011]*

Headstage gain	Unity (1x)
Input impedance	10^{14} Ω

Table 9.3: *RA16CH headstage [TDT, 2011]*

A/D	RA4PA: 4-channels 16-bit PCM RA16PA: 16-channels 16-bit PCM
Maximum Voltage In	+/- 4 millivolts
Frequency Response	3 dB 2.2 Hz - 7.5 kHz
Highpass filter	2.2 Hz
Anti-Aliasing Filtering	7.5 kHz (3 dB corner, 1st order, 6 dB per octave)
Input impedance	10^5 Ω
S/N (typical)	60dB

Table 9.4: *RA4PA/RA16PA pre-amp [TDT, 2011]*

Camera

A high-speed camera (Basler A602fc-2) operating at a framerate of 100 Hz was used to record locomotion of the rat. The camera was placed in front of the plexiglas cage containing the rat during locomotion. Adherent black markers were pasted on the skin of the rat on anatomical locations of the hindlimb (toe, hell, knee, hip and a reference). The camera was connected to the computer through a 10 pin RJ-45 jack and an IEEE 1394 socket connector. The camera was externally clocked through a connection to a DT340 card to synchronize video and TDT data. [Basler, 2010]

Treadmill

The motor-driven treadmill was enclosed in a plexiglas cover to prevent the rat from escaping during experiments. An adjustable back

Pixels	656 (H) x 490 (V)
Max. Frame Rate (at full resolution)	100 fps in 8 bit output modes

Table 9.5: *Basler A602fc-2 [Basler, 2010]*

wall was used to provide a running surface of at least 30 cm length and 10 cm width. Inclination of the treadmill was manually adjusted by use of a mini lifting jack and the angle was measured with a protractor. The treadmill was powered by a 12 V battery. To change the velocity of the treadmill a voltage divider and a resistor was used to alter the input voltage depending on behavioral task. Changing the inclination angle reduced the initial speed of the treadmill.

A treadmill speed of 29 $\frac{cm}{s}$ was decided in the light of studies by Gillis and Biewener [2001], where speed of rats were categorized in walk (17-48 $\frac{cm}{s}$), trot (59-71 $\frac{cm}{s}$) and gallop (60-122 $\frac{cm}{s}$).

Computer and software setup

Real-time Processor Visual Design Studio (RPvdsEx) running on a computer was used to communicate with the RX5 Pentusa Base Station (TDT system). The Vicon Motus 9.2 (Vicon Systems, Oxford, Great Britain) software was used to record the video data from the high-speed camera and afterwards for digitizing. All the data were stored on an external hard drive for later processing.

Electrodes

Selfmade intracortical electrodes and EMG electrodes were produced and implanted in the rats prior to recording. Surgical procedures are described in section 9.4 and manufacturing in Appendix C and Appendix D.

IC electrode design

IC electrodes were designed as depicted in Figure 9.2. Tungesten wire used for the electrodes had a diameter of 100 μm coated and 50 μm bare. The finished electrode covers an area of 2 mm x 2 mm with an internal distance of 2/3 mm.

This design was chosen on the basis of previous studies investigating mapping of the rat brain in stereotaxic coordinates [Leergaard et al., 2004].

9.3 Preparation of rats

Ten male Sprague-Dawley rats were trained for two weeks and the four best performing rats were selected for the experiment. After successful surgery, rats were individually caged and placed in a temperature controlled room with a 12/12 hour light/dark cycle. Food and water were available during all time in the cage.

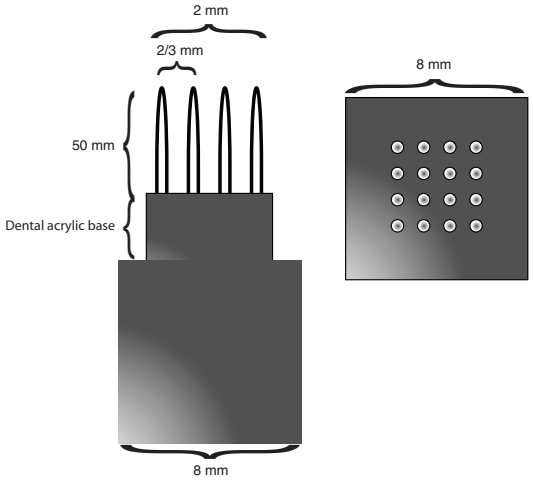

Figure 9.2: *Dimensions of the IC electrode from a side view (left) and top view (right). Diameter of the tungsten wire is 100 µm coated, 50 µm bare*

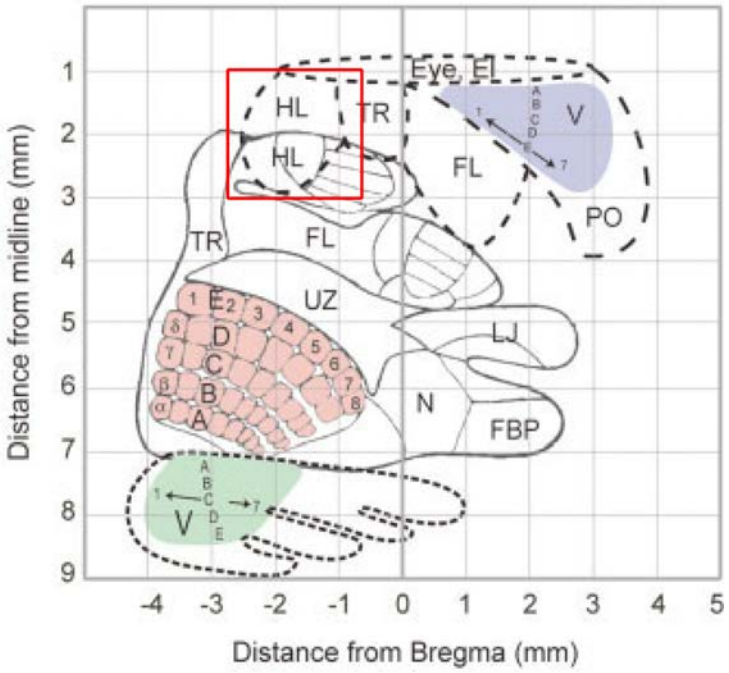

Figure 9.3: *Mapping of rat brain in stereotaxic coordinates. The hindlimb areas are approximately constituted by 2 mm x 2 mm (red square). [Leergaard et al., 2004]*

Performance of the rats was based upon observations and notes during training sessions. Being able to walk on the treadmill for at least 30 consecutive seconds was the inclusion criteria. This criteria was chosen in subject to reach sufficient gait cycles. The body mass of the rats had to be above 350 g the day of surgery to make sure the rats were fully developed before implementing electrode. The exper-

iment was carried out with approval from the Danish Committee for the ethical use of animals.

Hand training
The rats were hand trained for the first two days after arriving to the animal. This action was done in order to accustoms them to the new environment and human contact.

Treadmill training
Prior to the experiment the rats were trained on a treadmill for two weeks with two sessions a day.

For the initial training session the rats were placed on the treadmill for 10 minutes to get familiarized with the environment. The first time walking on the treadmill was with a low speed at 23 $\frac{cm}{s}$ to get the rat familiarized to walk on the treadmill. A training session on the treadmill consisted of 60 s trials with a break of 90 s in between. In case the rats received two training sessions per day a break of at least one hour was left between both sessions. If the rat performed good at a speed level of 23 $\frac{cm}{s}$ for the first session the speed level was increased in the next sessions. This was done until 29 $\frac{cm}{s}$ was reached as final speed level of the experiment. After the first week of training the rats was excluded from the experiment if they failed to run regularly (frequent immobility, stressful behavior or contact of the forelimbs on the treadmill walls). The different training tasks consisted of following:

- Locomotion on the horizontal treadmill with speeds ranging from 23 $\frac{cm}{s}$ to 29 $\frac{cm}{s}$.
- Locomotion on the treadmill with a 15^o inclination at speeds rangning from 23 $\frac{cm}{s}$ to 29 $\frac{cm}{s}$.

It was important that the rat had a steady locomotion to assure good video recordings for kinematic analysis. Notes and comments for each rat were noted to follow progression.

- Performance, estimated in seconds of steady running.
- Performance of the rat was rated with a grade, ranging from 0 (not running) to 6 (fluently running).

Markers
Adherent black markers were pasted on the skin of the rat on anatomical locations of the hindlimb and a reference point on the side. Markers included toe, heel, knee, hip and a reference, allowing segments to be made between toe-heel, heel-knee and knee-hip (Figure 9.4).

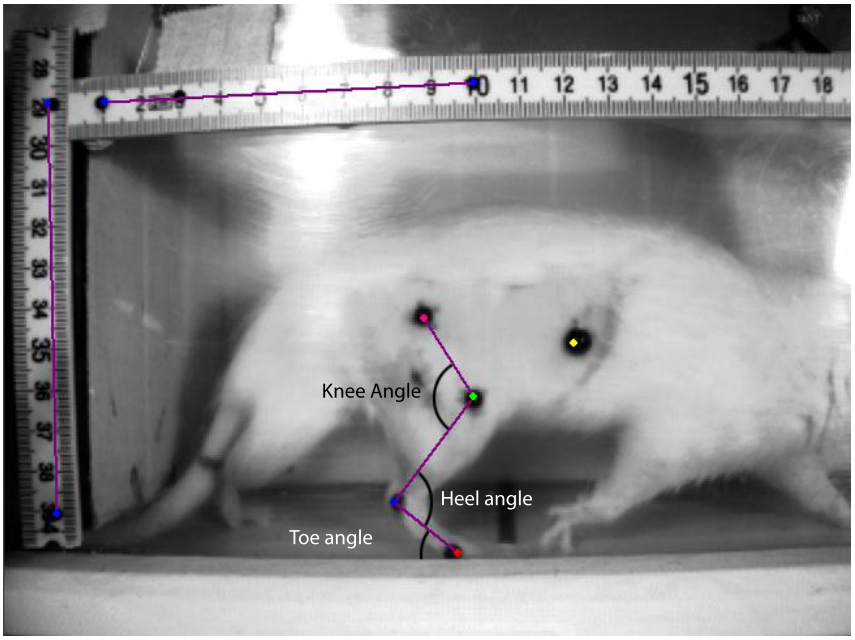

Figure 9.4: *Location of markers at toe, heel, knee, hip and a reference point on the side.*

9.4 Surgical procedures

Prior to recordings IC electrodes and EMG electrodes were implanted by a surgical operation. The surgery is divided into:

- Pre-operational preparations
- Preparation of the rats
- Implanting EMG electrodes
- Implanting IC electrode array
- Post surgery

List of materials

The following lists the materials used during surgery.

Workspace

- Non-sterile materials
  - Two tables with chairs
  - Microscope
  - Stereotaxic frame
- Sterile materials
  - Sterile fields
  - T-shirt (to cover microscope)

Surgeon

- Sterile materials
  - Masks and hats
  - Gloves

Preparation of rat

- Non-sterile materials
  - Shaver
  - Hypnorm/dormicum and sterile water (anaesthesia)
  - Lidocaine (local anesthetic)
  - Vaseline
- Sterile materials
  - Iodine sponge

Surgery tools and materials

- Non-sterile materials
  - Components for making cold-curing resins prosthetics (Heraeus Kulzer Paladur)
  - Cork boards
  - Sand bags
- Sterile materials
  - Towels
  - Gauze
  - Syringes
  - Sutures (size 4.0 and 5.0)
  - Spongostan (absorbable haemistatic gelatin sponge)
  - Saline
  - Aluminium tray
  - Cotton sticks
  - Rubber bands
  - LiquidBand Surgical S (surgical glue)
  - Scalpel
  - Clamps (curved)
  - Rongeur (for opening the skull)
  - Surgical spreader
  - Screw-driver
  - Drill
  - Needles
  - Ruler
  - Tissue forceps
  - Long forceps
  - Blunt scissors
  - Delicate scissors
  - Trocar
  - Bone screws with/without attached ground wires.
  - IC electrode
  - EMG electrodes

Part 1 - Pre-operational preparations

Sterilizing tools/materials and preparation of workspace were done prior to every operation. All tools to be sterilized (except IC- and EMG electrodes) were sterilized using an autoclave for steam sterilization. Tools were sterilized with a steam cycle of 3 min (steam)/3 min (dry) at 121^oC, whereas 10 min (steam)/10 min (dry) were used for towels and clothes. IC- and EMG electrodes were wrapped in green sterilization plastic bags and sterilized with gamma emission.

The operation room was organized with two tables, one being sterile and one non-sterile. The sterile table was covered with sterile fields and a sterile t-shirt was used to enclose the non-sterile microscope. A tray with sterile tools is placed at the sterile table and sand bags wrapped in sterile towels were put at the work area to support the rat (Figure 9.5).

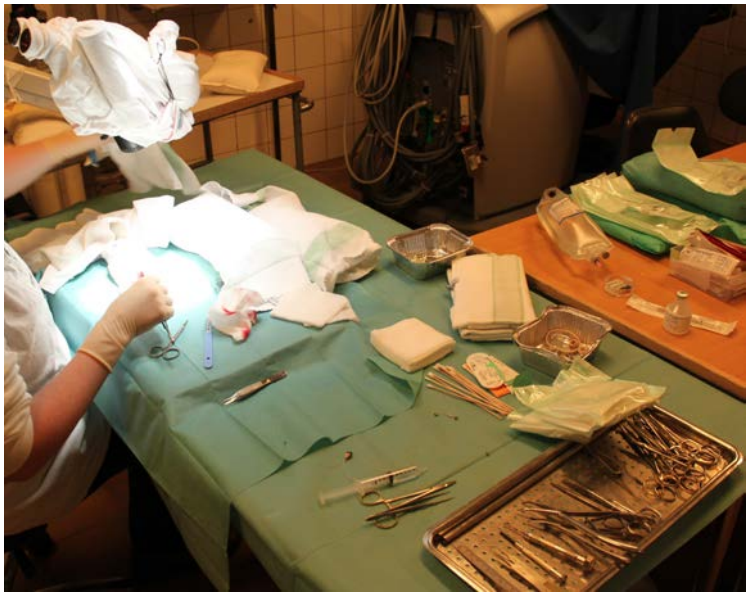

Figure 9.5: *The sterile and non-sterile table with tools and materials used during surgery.*

Part 2 - Preparation of the rats

The surgical procedure was performed under anaesthesia, which was maintained with a 0.02-0.03 ml Hypnorm (Fentanyl/fluanisone) and Dormicum (Midazolam) booster mixed with sterile water, when necessary. Level of anesthesia was monitored by checking the hindlimb withdrawal reflex on a regular basis. Every rat was weighed before surgery to estimate initial dosage. An initial dosage of 0.6 ml anesthesia was given and no more than 0.2 ml/100 g within the first hour of operation.

Shaving the skull and hindlimb was done after the rat was anesthetized by the initial dosage to expose the areas for implantation. The skin was prepared for surgery by use of an 1% iodine brush. Vaseline was applied to the eyes of the rat in order to prevent them from drying out during surgery (Figure 9.6).

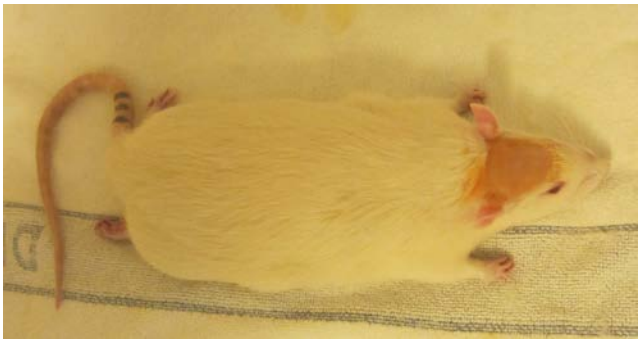

Figure 9.6: *Preparation of the rat before surgery. Shaving, cleaning skin with iodine and applying vaseline to the eyes.*

Part 3 - Implanting EMG electrodes

Description of the EMG electrode design and manufacturing can be found in Appendix D.

The rat was adjusted on the work area by using sand bags to support the body. An initial incision was made at the skull along the midline and another incision at the hindlimb for accessing biceps femoris and vastus lateralis. Separating the skin from the muscles in the hindlimb area was performed with use of a blunt scissor. A trocar was used to loosen the skin from the muscles and tunneling from the skull incision to the hindlimb incision before EMG electrodes were prepared and pulled through the tunnel from skull to hindlimb with help from a long forceps (Figure 9.7).

Electrodes were inserted into the muscles with use of needles and sutures. Extra wire was looped and attached to the hindlimb area to provide slack and preventing restriction of movement. Ground wires of different lengths from the electrodes were left under the skin in the tunnel. The incision at the hindlimb was stitched together and surgical glue applied, finishing up the EMG implantation (Figure 9.8).

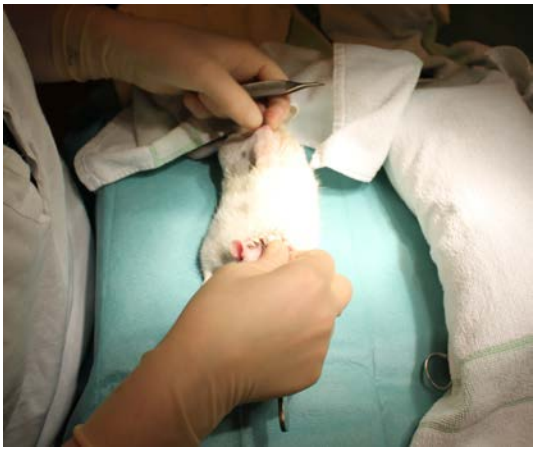

Figure 9.7: *Tunneling and pulling EMG electrodes through the tunnel were done with use of a long forceps.*

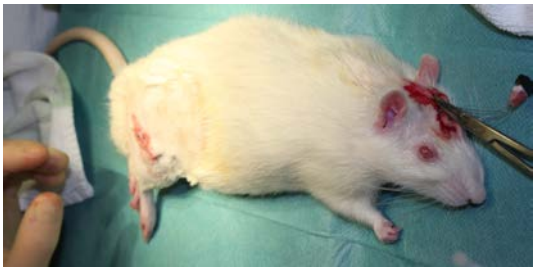

Figure 9.8: *Finishing up the EMG implantation by stitching together the hindlimb incision and applying surgical glue.*

Part 4 - Implanting IC electrode array

Description of the IC electrode manufacturing can be found in Appendix C.

The rat was fixated in a stereotaxic frame, lidocaine applied to the skin and ear bars of the frame and vaseline reapplied to the eyes. (Figure 9.9)

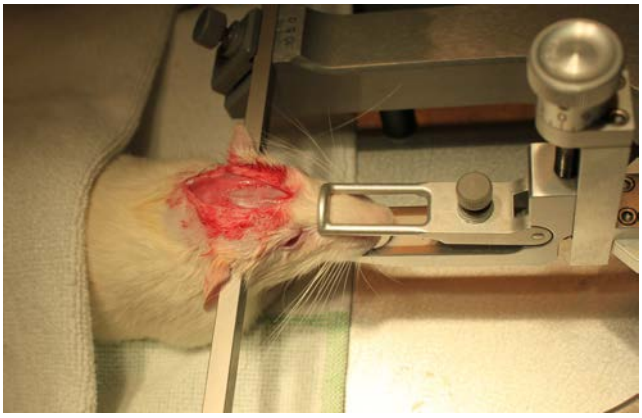

Figure 9.9: *Fixating the rat in a stereotaxic frame during IC implantation.*

The skull area was cleaned and the thin membrane covering the skull put aside. Four holes were drilled in the skull of the rat for inserting bone screws and allowing craniotomy with a hand drill of 2 mm diameter. A craniotomy was made with a rongeur above the primary motor cortex of the rat connected with the right hindlimb. The area for craniotomy was measured by use of the anatomical landmark, bregma, and the midline with a ruler and covered 3 mm x 3 mm, leaving some room for adjusting the implant site if blood vessels were blocking (section 9.2). Three screws were put in the remaining holes, whereas two of the screws had a ground connector attached. (Figure 9.10)

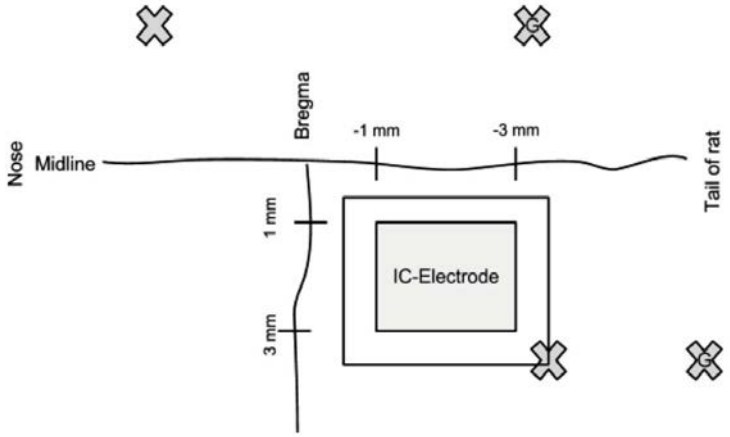

Figure 9.10: *Location of screw holes, screws with ground wires (G) and craniotomy area on the rat skull.*

Any sharp points at the edges of the craniotomy were removed and the membrane, dura, covering the brain was removed. This was done with a needle or scissor, exposing the area of motor cortex.

A dummy socket was inserted on top of the IC electrode ease the insertion process and provide a better overview during insertion. The IC electrode was fixated in a holder and navigated to the desired location with a micro manipulator on the stereotaxic frame. Lowering the electrode until the wires were resting on the surface ensured correct measuring of depth. A desired end depth for the electrode of 1.7 mm was obtained by quickly lowering the electrode 2 mm to penetrate followed by 0.3 mm retraction. (Figure 9.11)

Spongostan was put around the exposed motor cortex to prevent dental acrylic from reaching. Finally, dental acrylic was applied around the EMG- and IC connectors to finish up the surgery and eventually residue of acrylic were removed. (Figure 9.12)

Part 5 - Post surgery

After completed surgery, rats were returned to their cages and monitored the following days and given pain killers daily for 5 days. Rats

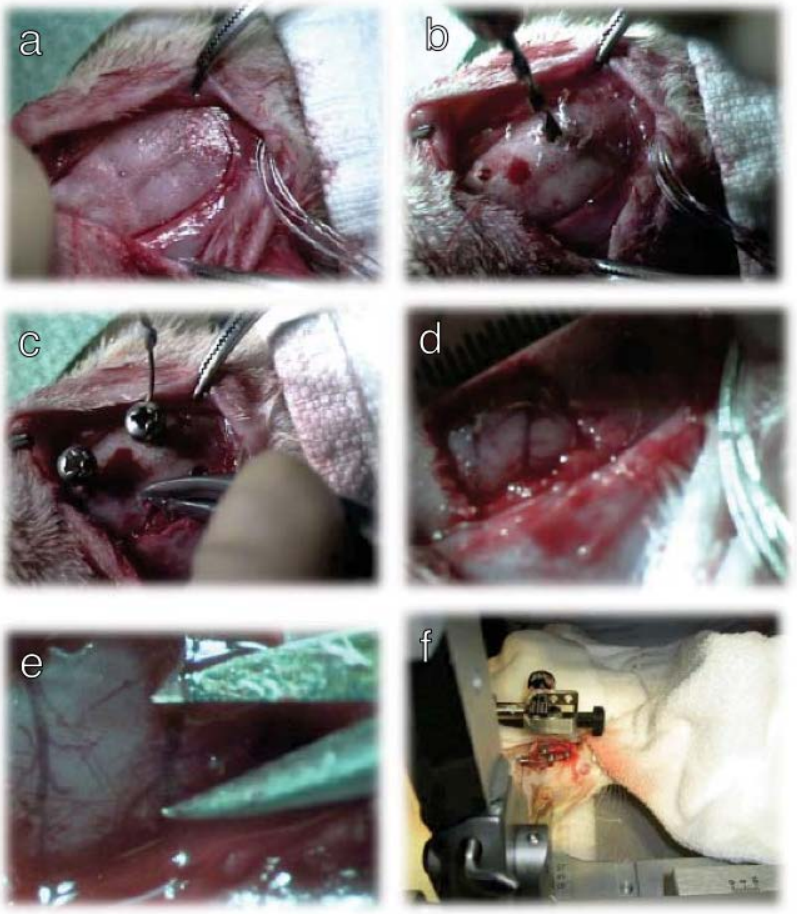

Figure 9.11: *a) Exposing the skull by retracting the skin and removing the membrane b) Drilling holes in the skull for bone screws and craniotomy c) Inserting bone screws and making the craniotomy d) Measuring the exposed area to ensure fit of the electrode e) Removing dura f) Inserting electrode*

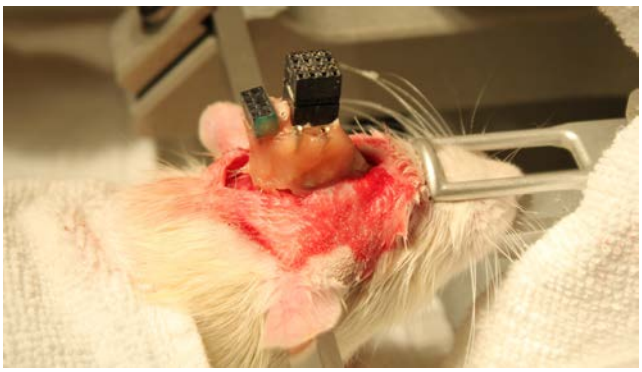

Figure 9.12: *Finishing up the surgery, applying dental acrylic around the connectors.*

were allowed a minimum of two days recovery before recording began.

9.5 Behavioral tasks

All rats included in the experiment were familiarized with a speed of 29 $\frac{cm}{s}$ and had undergo treadmill training for two weeks. Each task consisted of walking on the treadmill at 29 $\frac{cm}{s}$ without inclination or with 15^o inclination. These tasks were chosen to examine any differences in modulation of IC or EMG signals of the rats. Each task was completed four times with a break of 4 min in between to minimize fatigue. Each recording session was ended with a steady recording with the treadmill turned off.

9.6 Data acquisition

IC microstimulation

Microstumulation of the IC electrode array was performed two-three days after successful surgery. The aim for stimulation was to identify which channels corresponded to the hindlimb area in M1.

Each of the 16 channels was stimulated with a start current of 100 μ A and increased in steps of 100 μ A until a maximum of 500 μ A was reached. Stimulation current was decreased with 50 μ A If any response was observed to find the lowest threshold current necessary to generate muscle contraction in the hindlimb. [Jensen et al., 2006; Neafsey et al., 1986]

Applied current and responses, if any, were noted down and available in Appendix E

Control recordings

A control recording of 30 s video at a speed of 29 $\frac{cm}{s}$ without inclination was recorded for all rats prior to surgery. This step was taken to identify possible alterations of normal gait due to the surgical procedures.

IC recording

IC signals were recorded using a 16 channel fine-wire electrode array located in the hindlimb area of motor cortex. The recordings was made using an automatic threshold of RMS of the signal multiplied by 1.2. Waveforms of action potentials and corresponding time stamps (snippets), when the automatically threshold was exceeded, were sampled at 24.414 kHz and bandpass filtered (LP: 8000 Hz, HP: 800 Hz) and stored as snippets of spike activity.

EMG recording

EMG was recorded in a bipolar configuration from chronic implanted electrodes in the biceps femoris and vastus lateralis in the right hindlimb. The continuous EMG signal was sampled at 4882.8 Hz and

bandpass filtered (LP: 2500 Hz, HP: 20 Hz).

Video recording

Video recordings of the rats were recorded with a Basler A602fc-2 high speed camera. Video recordings were made in order to synchronize EMG and IC activity and analyzing kinematics of gait. Recordings were in addition used to compare with control recordings to detect if any alteration of gait occurred due to surgery.

9.7 Storing data

Data from EMG-, IC-, synchronization signals and kinematics/angles (described later) are stored in a MATLAB struct for easy access (Figure 9.13).

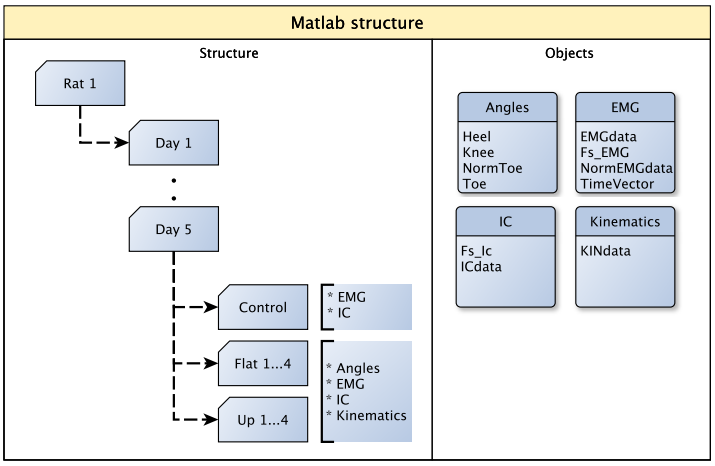

Figure 9.13: *The MATLAB structure for storing data for each rat in order to ease the data import and analysis in MATLAB. Variable names for each object are shown to the right.*

CHAPTER 10

Signal processing and data analysis

This chapter describe the steps of data processing, data analysis and building a decoding model. Analysis of data are divided into three different parts: video recordings, intracortical signals and EMG signals. Analysis of data aims to characterize recorded signals and process features and information to feed as appropriate I/O for an ANN.

10.1 Artificial Neural Network strategy

An ANN is utilized for prediction of muscle activity on the basis of neural activity recorded from M1. ANN in general is explained in Appendix B. Initial configuration of the ANN is based on previous studies by Sanchez and Principe [2007]; Wessberg et al. [2000]:

- Feedforward network
- Single hidden layer
- 15-20 neurons
- Powell-Beale conjugate gradient training algorithm

Due to the fact of a limited amount of hindlimb associated channels (Appendix E), different approaches of ANN inputs will be tested. The data sets (individual channels) will be divided into two categories being dependent on results from microstimulations:

- Group A: Channels associated with hindlimb
- Group B: Channels with visible modulations in PSTH's

Evaluation and analysis of the data are performed before channels of Group B are selected (described in section 10.2).

10.1.1 Analysis of video recordings

All video recordings from the behavioral tasks were digitized by tracking the coordinates of the attached markers (chapter 9). A total of nine points were tracked (x1, x2, y1, y2, toe, heel, knee, hip, ref), whereof the cage markers x1, x2, y1 and y2 were stationary points.

Raw XY-coordinates for each point were saved and imported as *KIN-data* to the MATLAB struct for the corresponding rat (Figure 9.13). If the markers for any reasons were not visible, e.g. if the foot marker was hidden under the back wall, a fictive point was chosen resulting in clearly identifiable outliers when calculating angles. (Figure 10.1)

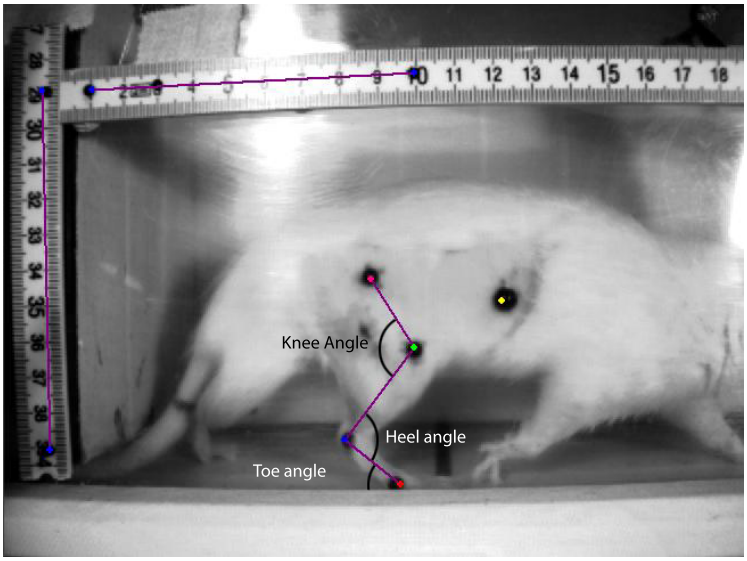

Figure 10.1: *Tracking the nine markers in Vicon Motus. Joint angles are presented in the figure.*

10.1.1.1 Kinematics

The raw digitized XY-coordinates were imported into MATLAB and joint angles for knee, heel and toe are calculated by generating segments from the XY-coordinates (Figure 10.1).

Angles were plotted and inspected for any characteristics revealing unique parts of the gait cycle. By finding the peaks and valleys for each angle indicated a lift-off time could be correlated with the peak of the toe angle. This angle showed a consistent pattern with very distinguishable peaks (Figure 10.2).

Inspection of different peaks within the toe angle and manually comparing with the video recordings, indicated a convergence between lift-off and location of peaks.

Durations of gait cycles were calculated after retrieving all index-values for lift-off. This duration, together with joint angles, were used to set up criteria for inclusion and exclusion of gait cycles.

Location of toe-down was detected by finding the valleys within x-coordinate of toe marker movement. X-coordinate of the toe marker was subtracted from the x-coordinate of the reference marker in order to normalize and make a smooth plot (Figure 10.3). Inspection of different peaks within the x-coordinate and manually comparing with the video recordings, indicated a convergence between toe-down and location of valleys.

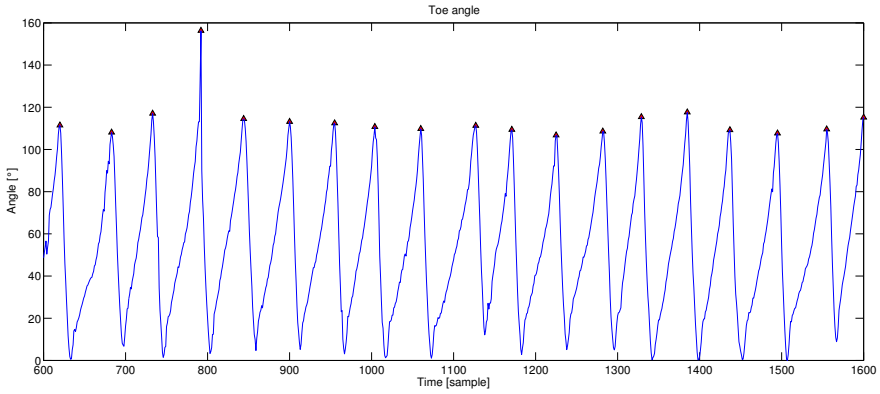

Figure 10.2: *A segment of the angular changes at the toe during a behavioral task. Locations of angular peaks are detected and saved in MATLAB. An example of angular outlier is shown.*

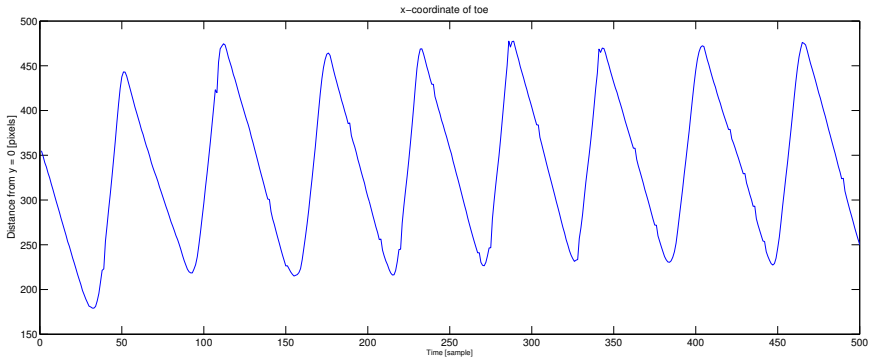

Figure 10.3: *A segment of the x-coordinate changes of the toe marker during a behavioral task. Locations of peaks are detected and saved in MATLAB.*

Criteria for good gait cycles

Defining a good gait cycle was important in order to have well characterized signals as input to the ANN.

Duration time of the gait cycles varied accordingly to the behavior of the rat on the treadmill. By manual inspection of the videos it was found, getting stuck under the back wall resulted in fast short gait cycles and standing still on the treadmill without moving returned a very long gait cycle.

Mean gait duration was calculated for each rat for two different days and mean duration was compared. The criteria for a good gait cycle was decided to be 55 frames ±15 frames (1 frame = 10 ms).

Visual inspection of the angular range for the joint angles was done by plotting cyclograms. The cyclograms revealed a range from 80^o-125^o (knee) 0^o-120^o (toe) 20^o-100^o (heel) (Figure 10.4 and Figure 10.5). Gait cycles with joint angles exceeding these ranges were excluded

as input for the ANN. Index of gait cycles fulfilling the requirements were saved for further analysis.

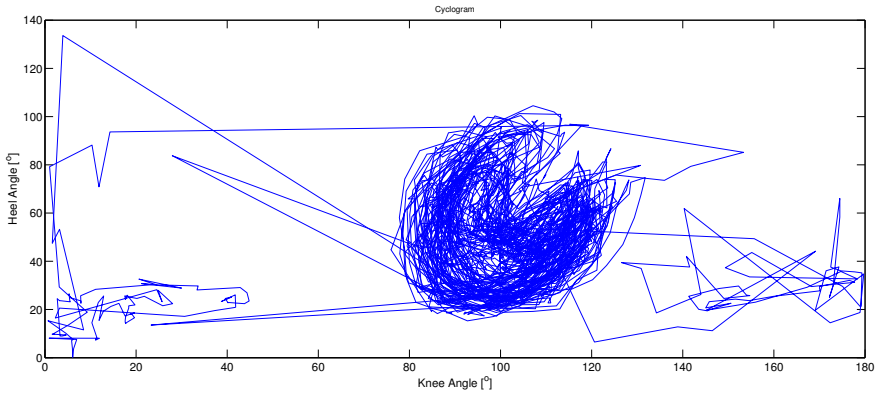

Figure 10.4: *Cyclogram illustrating the coordination between knee and hip of the right hindlimb.*

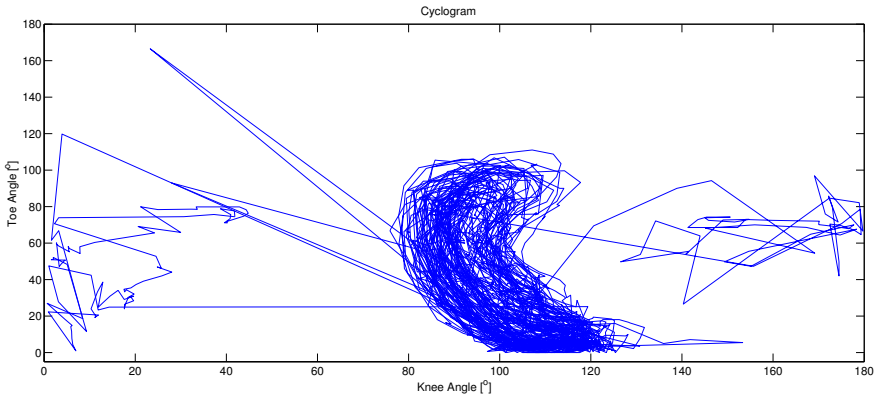

Figure 10.5: *Cyclogram illustrating the coordination between knee and toe of the right hindlimb.*

10.1.2 Preprocessing of intracortical signals

The interesting information, when analysing intracortical signals, were the timing of the action potentials firing. An easy way to visualize the firing of neurons were by inspecting a raster plot. The raster plot substitute the time when the threshold are exceeded with a tick, which is done for each event time.

Peri-stimulus time histograms were then made to retrieve an average neural response centered around the event time. Timings from the raster plot were summarized in windows (bins) of desired size.

PSTH's of neural activity during gait cycles from lift-off to lift-off were calculated for each session of behavioral tasks within a dynamic bin-size ranging from 1% of gait durations from 40-70 samples according to mean duration (bin-sizes ranging from 8.33 ms to 11.66 ms)

due to normalization. PSTH's were normalized in percentage of gait cycle according to the mean duration. An example of PSTH's calculated for each channel of the IC electrode are depicted in Figure 10.6 with a bin-size normalized in regard to percentage of gait cycle. Mean values for each PSTH were subtracted in order to normalize the diagrams and omit high background activity.

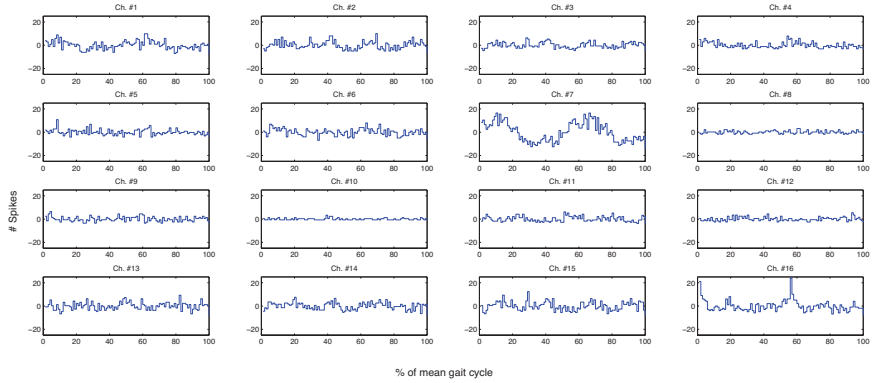

Figure 10.6: *An overview of neural activity for all 16 IC channels. Normalized to percentage of full gait cycle, according to the mean duration of gait cycles. Channel 1, 2, 3, 4, 7 and 9 showed hind limb responses according to micro stimulation.*

An envelope was made by using a moving average filter with window length of 5 samples. This envelope was plotted to see any tendencies in modulation due to gait (Figure 10.7). The PSTH's are used as feature for input to the ANN.

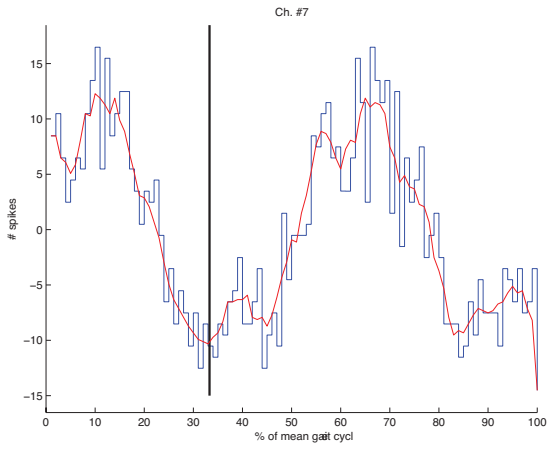

Figure 10.7: *PSTH from channel 7 corresponding to hindlimb activity. An envelope is plotted (red) to visualize tendencies in modulations and toe down is marked with a vertical black line.*

10.1.3 Preprocessing of EMG signals

A few large spikes appear in the raw EMG-signal, for which reason a band-pass filter (20-500 Hz) was applied to reduce spikes but still maintain the shape of the EMG. Furthermore a band-stop filter was applied (49.5-50.5 Hz). Signals from the two recording sites within the two muscles were subtracted to retrieve the actual signal due to the bipolar configuration. Full-wave rectification of the signals were done before normalization in terms of maximal EMG value is calculated. An outline of muscle activity was visible for each muscle, vastus lateralis in particular (Figure 10.8 and Figure 10.9). A small initial burst of VL seemed to be visible in the rectified signal and more distinct in the envelope (Figure 10.11). This was in agreement with findings of Gillis and Biewener [2001]. The envelope was made by a 5 Hz low-pass filter.

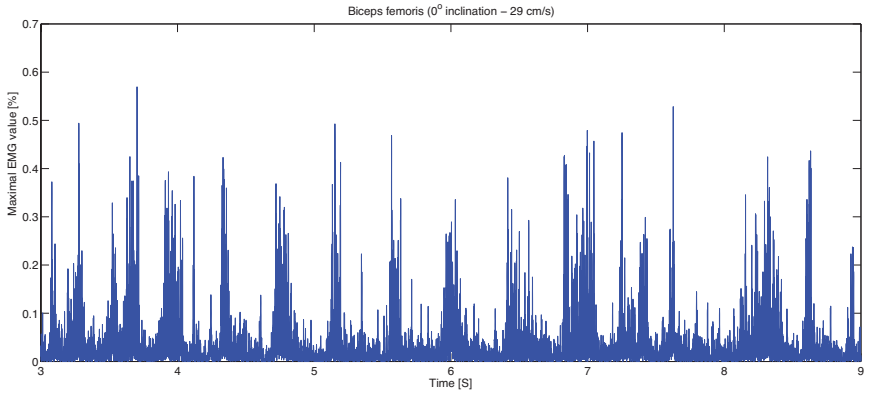

Figure 10.8: *Full-wave rectified EMG signal from biceps femoris. EMG signals are normalized according to maximal EMG value.*

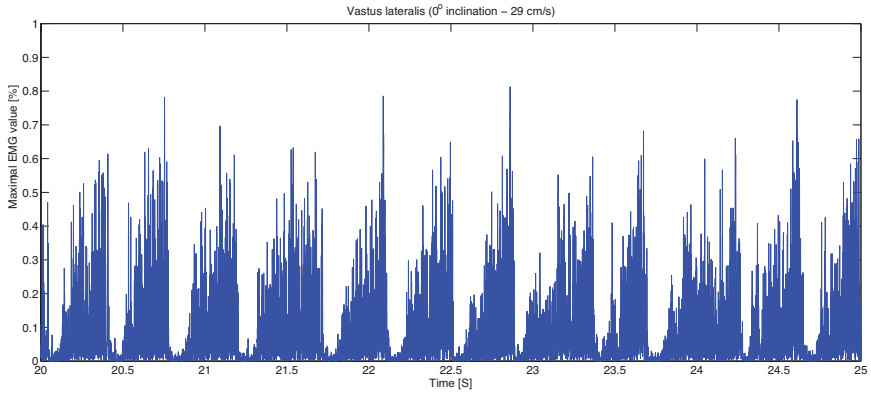

Figure 10.9: *Full-wave rectified EMG signal from vastus lateralis. EMG signals are normalized according to maximal EMG value.*

Calculating the mean maximal EMG value for both muscles for each behavioral task indicated a general pattern with vastus lateralis be-

ing the primary active muscle during gait, compared with biceps femoris. Furthermore, mean maximal EMG value levels increased significantly for biceps femoris in rat 1 for recordings with 15^o inclination compared with horizontal (Table 10.1 and Table 10.2).

	Rat 1	
	Biceps femoris	Vastus lateralis
Horizontal	0.0420 (SD ± 0.0055)	0.1087 (SD ± 0.0056)
Inclination	0.0693 (SD ± 0.0047)	0.1109 (SD ± 0.0060)

Table 10.1: *Mean values of normalized EMG for rat 1.*

	Rat 2	
	Biceps femoris	Vastus lateralis
Horizontal	0.0601 (SD ± 0.0055)	0.0395 (SD ± 0.0054)
Inclination	0.0697 (SD ± 0.0064)	0.0449 (SD ± 0.0037)

Table 10.2: *Mean values of normalized EMG for rat 2.*

Index-values for good gait cycles (subsubsection 10.1.1.1) were used to extract corresponding EMG-activity from lift-off to lift-off (full-wave rectified) for further conditioning. A low-pass filter (5 Hz Butterworh) was applied to get an envelope of the EMG (Figure 10.10 and Figure 10.11). A downsampling of the envelope are performed with a moving average filter with a window length of variable samples, since an ANN expects input and output of same length. The mean of downsampled EMG was calculated and consisted of 100 values corresponding to the 100 PSTH bins. Mean EMG activity were used as feature for output of the ANN. Input-output relation for the ANN model is depicted in Figure 10.12.

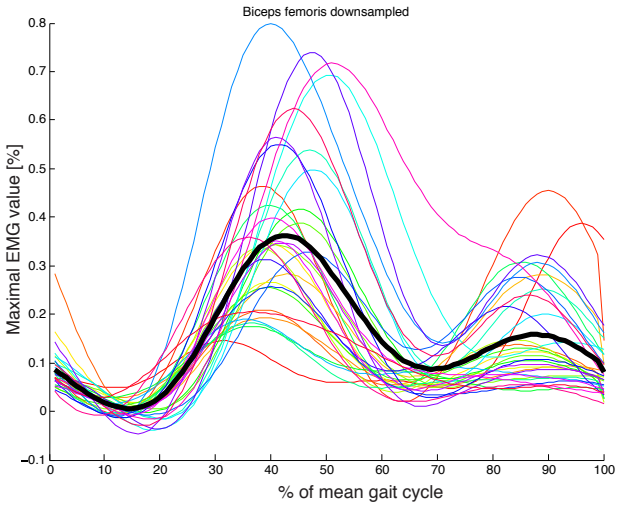

Figure 10.10: *Envelope of EMG-signals for biceps femoris, fulfilling the requirements for a good gait cycle from rat 1. Mean activity is outlined in black.*

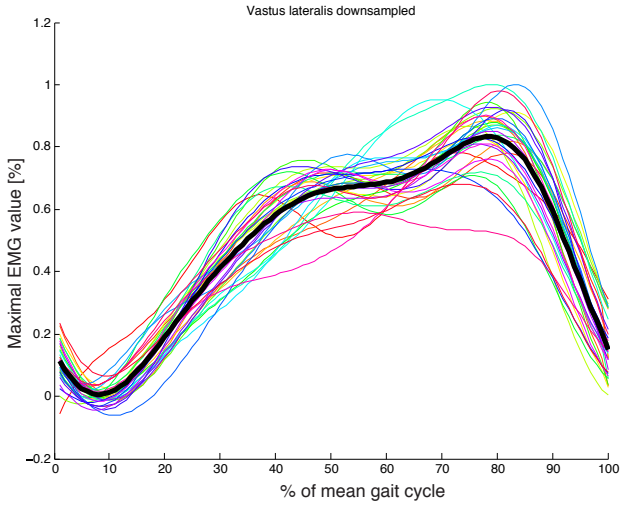

Figure 10.11: *Envelope of EMG-signals for vastus lateralis, fulfilling the requirements for a good gait cycle from rat 1. Mean activity is outlined in black.*

10.2 Artificial Neural Network

Designing a Neural Network is divided into the following steps below.

1. Collect data
2. Create the network
3. Configure the network
4. Initialize the weights and biases
5. Train the network

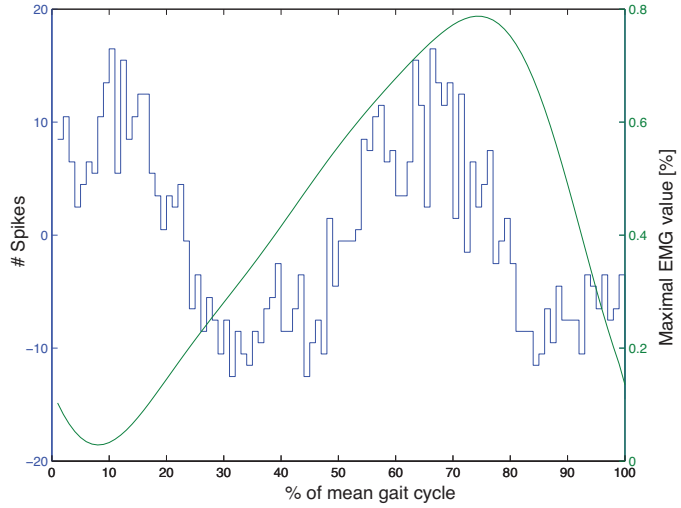

Figure 10.12: *Syncronized PSTH from hindlimb channel 7 with the corresponding mean muscle activity of vastus lateralis.*

These steps will be examined individually in this section by use of the Neural Network Toolbox ^{TM} User's Guide [Beale et al., 2012].

Step 1 - Collect data

Five days of recordings was performed on each rat with four sessions for each task per day. Due to missing event detections from IC recordings, several sessions had to be excluded and the total amount of available sessions for data analysis is shown in Table 10.3.

	Sessions available
Rat 1	
Horizontal walking	16
Inclined walking	16
Rat 2	
Horizontal walking	12
Inclined walking	7

Table 10.3: *The table show the amount of sessions available for each rat.*

Extraction of features (PSTH and EMG) used for the ANN are described in subsection 10.1.2 and subsection 10.1.2. Normalization of the data are critical when preparing the data, since the network will not be better than the data it is trained on, due to lack of ability to extrapolate beyond the input range.

Data are split in subsets of training data and validation data, in order to train and monitor the performance. The ANN is configured to randomly divide input data into training/validation sets of ratio 70/30.

Division of data

Channels for Group A are based on microstimulation responses of the hindlimb, yielding:

- Rat 1 Group A: 1, 2, 3, 4, 7, 9
- Rat 2 Group A: 2, 3, 8

Due to the low amount of channels resulting in hindlimb responses from micro stimulation, further investigation of the remaining channels were done. Distinct activation patterns were observed in some channels which were consistent across days and sessions(Figure 10.13) compared to other channels without hindlimb responses(Figure 10.14). The channels with distinct activation patterns are all located within the hindlimb area of the motor cortex documented by [Leergaard et al., 2004], and are therefore included in the group B as potential channels with hindlimb associations.

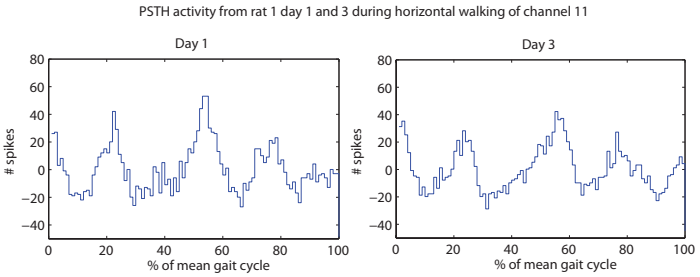

Figure 10.13: *PSTH activity from action potential firing from channel 11(Group B) in rat 1 day 1 and 3 during horizontal walking.*

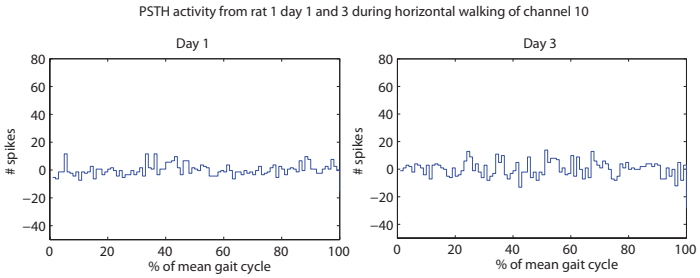

Figure 10.14: *PSTH activity from action potential firing from channel 10 in rat 1 day 1 and 3 during horizontal walking.*

- Rat 1 Group B: 11,16
- Rat 2 Group B: 6,7,11

Different combinations of ANN models are created to evaluate and find the best performing network, measured by the coefficient of determination for predictions. A model will be created for each rat with the following cases:

- **Case 1:** Use 1 day of horizontal recordings to test model trained on the remaining 3 days of horizontal.
- **Case 2:** Use 1 day of inclined recordings to test model trained on the remaining 3 days of incline.
- **Case 3:** Use all days of horizontal to test model trained on all days of inclined data.
- **Case 4:** Use 1 day of horizontal and incline to test model trained on the remaining day.

Step 2-4 - Create, configure and initialize the network

A multilayer feedforward net (fit net) with 20 neurons in a single hidden layers, able to map input/output relations, is used for the problem. A Conjugate gradient backpropagation with Powell-Beale restarts is used as training function with transfer function being tan-sigmoid in the hidden layer and linear transfer function for the output layer. Before training the weights of the network are initialized.

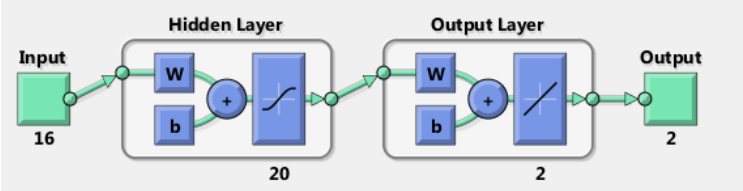

Figure 10.15: *Configuration of the ANN.*

Step 5 - Train the network

The artificial Neural Network is trained and re-initialized 10 times to get the best R^2 value as possible, since weights and bias changes for every initialization. The ANN specifications used for prediction by Wessberg et al. [2000] was trained with the data from the experiment, where neural activity were used as input and EMG data as output

With the same ANN specifications used in Wessberg et al. [2000] the data from the experiment was used for training the ANN model, with neural activity as input and EMG activity as output. The ANN was tested with input from group A, B and AB. The output was provided to the ANN with EMG activity from biceps femoris and vastus lateralis and the results are shown in Table 10.4.

The ANN results from Wessberg et al. [2000] showed R^2 values ranging from 0.2025-0.6241 which are high compared to the R^2 values from the prediction with the experimental data of 0.1020 for biceps femoris and 0.0002 for vastus lateralis (Figure 10.16 and Figure 10.16).

Improvements of the ANN is therefore necessary in order to optimize the performance. This can be accomplished by trying different configurations of the ANN.

	Biceps femoris	**Vastus lateralis**
A	0.0795	0.0181
B	0.0268	0.0159
AB	0.0975	0.0197

Table 10.4: *R^2 values obtained by the model for different test groups and different muscles.*

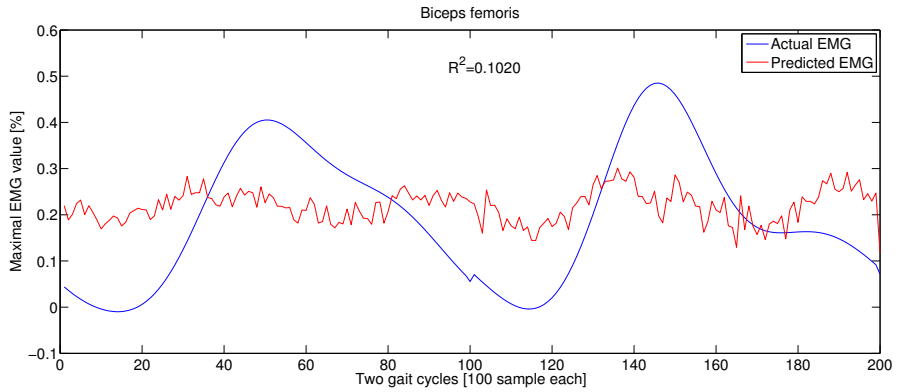

Figure 10.16: *Prediction of biceps femoris from the AB experimental data with settings from Wessberg et al. [2000].*

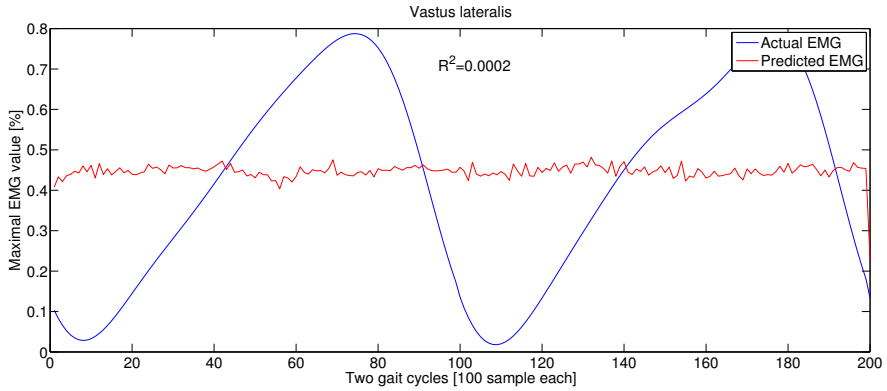

Figure 10.17: *Prediction of vastus lateralis from the AB experimental data with settings from Wessberg et al. [2000].*

CHAPTER 11

Optimization of Artificial Neural Network

Optimization of the ANN was needed in order to achieve a better prediction of muscle activity from the data sets. Optimization of the ANN model can be subdivided into the parts: optimization of configuration and parameters of the ANN, optimization of input-data and optimization of output-data.

11.1 Strategy

To optimize the performance of the ANN network, a systematical approach was decided. Each part of the optimization (ANN configuration, input and output) was evaluated individually before moving on.

Results obtained by initial training (Table 10.4) were used as references, in order to evaluate and test the performance of the ANN. Prediction of a single muscle was chosen in order to simplify the optimization process. Evaluating the results in Table 10.4 yield a better prediction for biceps femoris regardless of division of data. The AB group is chosen since the model gave the highest R^2 values.

Re-initialization of the model was done 10 times for each change, since the initial bias and weights determined the end results. The best R^2 value of the 10 iterations was saved as the final result

Initial configuration of the ANN:

- Group: AB
- Muscle: Biceps femoris
- Hidden layers: 1
- Neurons: 20
- Training function: Conjugate gradient backpropagation (Powell-Beale restarts)

To test the final optimized configuration of the ANN and evaluate capabilities to generalize across behavioral tasks, several cases were tested:

- **Case 1:** Use 1 day of horizontal recordings to test model trained on the remaining 3 days of horizontal.

- **Case 2:** Use 1 day of inclined recordings to test model trained on the remaining 3 days of incline.
- **Case 3:** Use all days of horizontal to test model trained on all days of inclined data.
- **Case 4:** Use 1 day of horizontal and incline to test model trained on the remaining day.

11.1.1 Part 1 - optimization of ANN configuration

The easiest way to optimize the results was by tweaking the ANN configuration. Adjusting the amount of neurons and number of hidden layers seems obvious, since increasing these parameters would enable the ANN to encounter more complex data sets and enhance the linearity of the data. [Beale et al., 2012; Sanchez and Principe, 2007]

Combinations of layers ranging from 1 to 5 and number of neurons from 10 to 50 were tested. Results are shown in Table 11.1.

	1 layer	**2 layers**	**3 layers**	**4 layers**	**5 layers**
10 neurons	0.1044	0.131	0.1148	0.1225	0.1084
20 neurons	0.1271	0.1229	0.1167	0.1147	0.1412
30 neurons	0.1384	0.1336	0.1307	0.1281	0.1263
40 neurons	0.1337	0.1370	0.1572	0.1542	0.1192
50 neurons	0.1224	0.1370	0.1264	0.1410	0.1440

Table 11.1: *Performance of the model in R^2 values with combinations of hidden layers and neurons.*

Highest R^2 values were obtained with 3 hidden layers consisting of 40 neurons. Memory usage and training time increase significantly, when changing amount of neurons and hidden layers. Results of this configuration is seen in Figure 11.1.

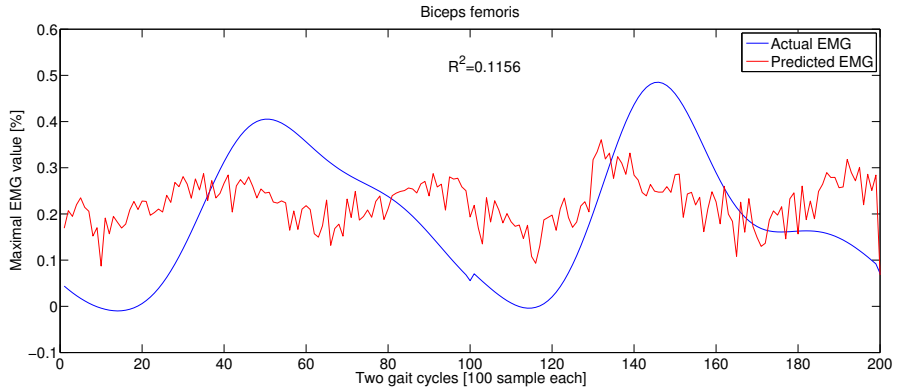

Figure 11.1: *Prediction of biceps femoris from the AB experimental data with 3 hidden layers and 40 neurons.*

The last essential parameter of the ANN was the training function. According to several studies (Sanchez and Principe [2007]; Wessberg

et al. [2000]) backpropagation algorithms were recommended. Matlab offer an extensive list of backpropagation training algorithms, of which several were chosen and tested (Table 11.2). Different training functions could be used for the ANN and varies in computation speed, memory usage and efficiency depending on size of data sets. Choosing a single training function could therefore be difficult and must be adjusted according to desired goal (optimal speed, memory usage or efficiency). [Beale et al., 2012]

	R^2
Levenberg-Marquardt backpropagation	0.2237
Conjugate gradient backpropagation (Powell-Beale restarts)	0.1572
Bayesian Regulation backpropagation	0.1466
RPROP backpropagation	0.1396
Scaled conjugate gradient backpropagation	0.1352
One step secant backpropagation	0.1252
Gradient descent w/momentum & adaptive lr backpropagation	0.0984
Gradient descent backpropagation	0.0416

Table 11.2: *R^2 values obtained by the model for different training algorithms.*

The trade-off for this value was training speed being >3 hours. The four best performing algorithms were kept for further optimization. Results from Bayesian Regulation backpropagation, Levenberg Marquardt backpropagation, Conjugate gradient backpropagation and RPROP backpropagation are shown in Figure 11.2, Figure 11.3, Figure 11.1 and Figure 11.4.

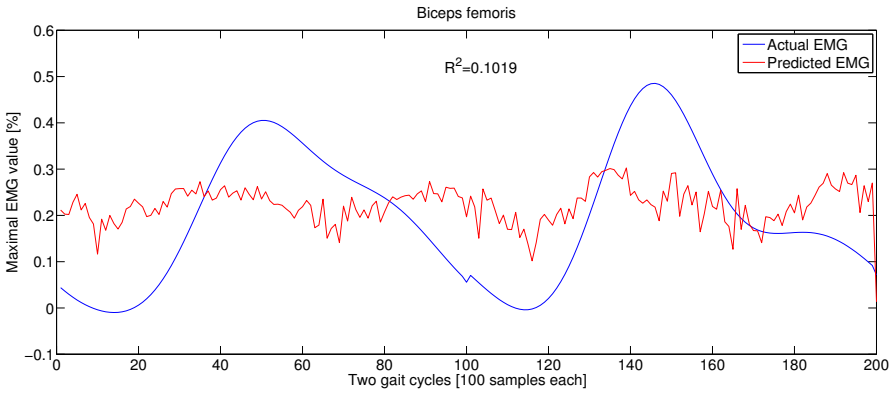

Figure 11.2: *Prediction of biceps femoris from the AB experimental data with 3 hidden layers, 40 neurons and Bayesian Regulation backpropagation training algorithm.*

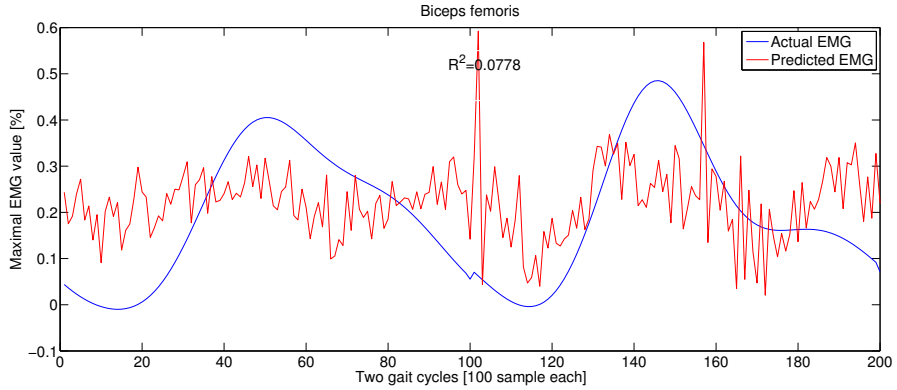

Figure 11.3: *Prediction of biceps femoris from the AB experimental data with 3 hidden layers, 40 neurons and Levenberg-Marquardt backpropagation training algorithm.*

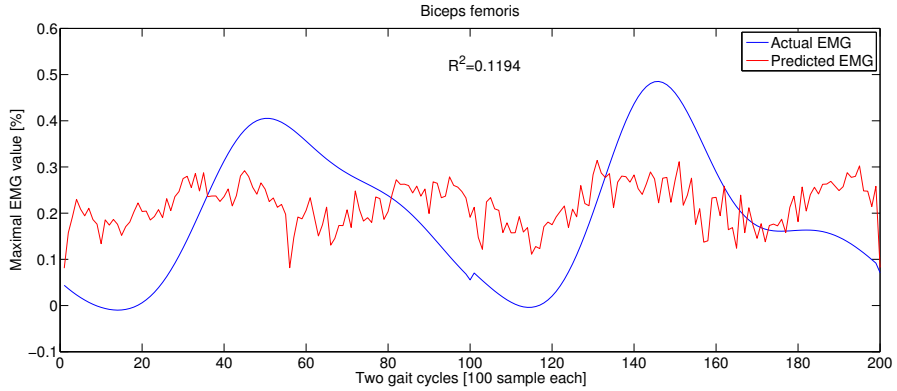

Figure 11.4: *Prediction of biceps femoris from the AB experimental data with 3 hidden layers, 40 neurons and RPROP backpropagation training algorithm.*

Highlight

- Group: AB
- Muscle: Biceps femoris
- Hidden layers: 3
- Neurons: 40
- Training function(s):
  - Bayesian Regulation backpropagation (BR)
  - Levenberg-Marquardt backpropagation (LM)
  - RPROP backpropagation (NRP)
  - Conjugate gradient backpropagation (CGB)

The standard ANN training function, and recommended first choice was LM which had good performance and generally the fastest training function with a low mean square error, though with a high memory usage. [Beale et al., 2012]

11.1.2 Part 2 - optimization of input data

Next step included optimization of the input data, which for the ANN model was PSTH's. Shape of the PSTH's were dependent on the bin-size of the plots. Changing the size, and thereby resolution, could alter possible modulation patterns visible in the PSTH. Bin-sizes of 0.5%, 1%, 2% and 5% were tested (Table 11.3).

	NRP	CGB	LM	BR
0.5%	0.1818	0.0825	0.1188	-
1%	0.1396	0.1572	0.2237	0.1466
2%	0.1925	0.1950	0.3028	-
5%	0.3044	0.2825	0.5774	-

Table 11.3: *R^2 values obtained by the model for different bin-sizes and training functions.*

The BR function does not use an early stop criteria but Bayesian regularization, giving a better generalization performance. Since the validation data were not separated from the training data and all data were analyzed, a heavy computation time was needed due to the large amount of iterations (>8 hours) [Beale et al., 2012]. Therefore the BR function was discarded and only trained with a bin-size of 0.5%. LM was chosen as the optimal choice with a bin-size of 5%. Results are seen in Figure 11.5.

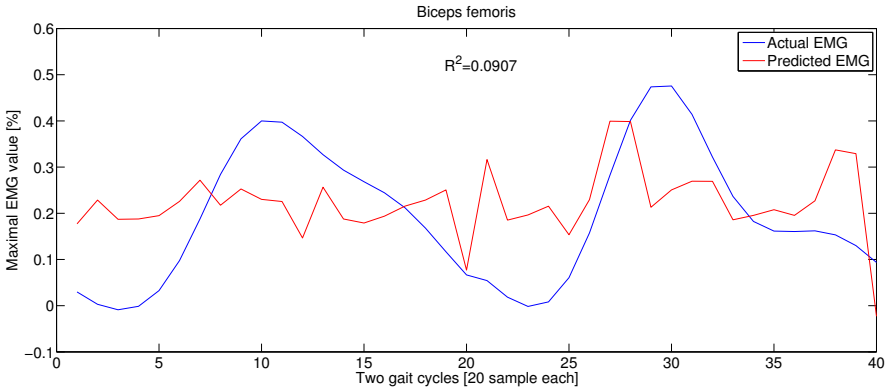

Figure 11.5: *Prediction of biceps femoris from the AB experimental data with 3 hidden layers, 40 neurons, bin-size of 5% and LM training algorithm.*

Beside the bin-size, inclusion criteria for gait durations might have affected the outcome. Different durations were tested in order to evaluate the affect of gait durations. Beside the original range of 0.4 s to 0.7 s, 0.45 s to 0.65 s and 0.50 s to 0.60 s were tested (Table 11.4).

The results from testing different gait durations did not reveal any advantages of changing the original duration interval. Further conditioning of the input PSTH was filtering with a moving average filter

	R^2
50-60	0.3849
45-65	0.3613
40-70	0.5774

Table 11.4: *R^2 values obtained by adjusting criteria for gait durations included.*

of different spans. Strong fluctuations were eliminated or reduced by filtering the PSTH. Spans of 5, 10, 15 and 20 samples were tested. In addition a time-delay of the EMG signal existed, due to the fact that neural activity were recorded and occur before any effects were seen in the EMG. Different shifts of the EMG were for that reason tested together with smoothing of the signal (Table 11.5).

	0 samples	**5 samples**	**10 samples**	**15 samples**	**20 samples**
0%	0.5774	0.7274	0.6583	0.5943	0.5881
5%	0.4351	0.6281	0.5501	0.5260	0.6022
10%	0.3863	0.6406	0.6493	0.5970	0.5715
15%	0.3699	0.5829	0.5885	0.4858	0.5906

Table 11.5: *R^2 values obtained with different spans of a moving average filter and shifting of the EMG.*

Reducing the time-delay between neural activity and EMG did not seem to have a positive effect for the prediction, if no smoothing was applied. Performance at 5 sample window stood out and results are shown in Figure 11.6.

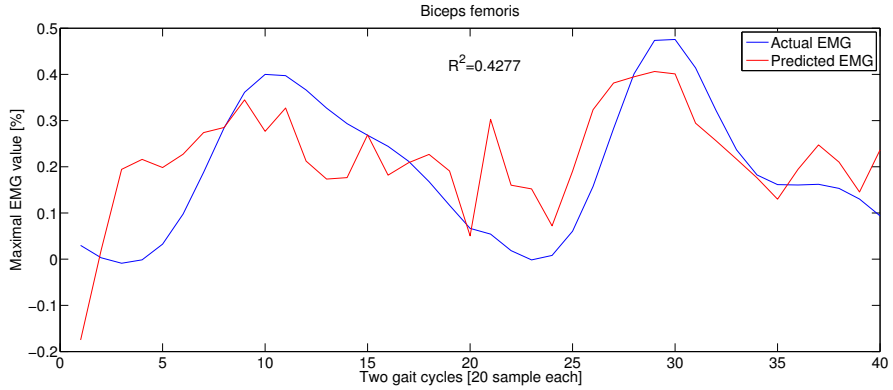

Figure 11.6: *Prediction of biceps femoris from the AB experimental data with 3 hidden layers, 40 neurons, bin-size of 5%, LM training algorithm and a moving average filter with 5 samples span.*

The optimal configuration so far:

- Group: AB
- Muscle: Biceps femoris
- Hidden layers: 3
- Neurons: 40
- Training function: Levenberg-Marquardt backpropagation (LM)
- Bin-size: 5%
- Shifting: 0%
- Moving average span: 5 samples

11.1.3 Part 3 - optimization of output data

After an optimization of input data, the last step was optimization of the output data. Using FES in practice rely on the ability to detect whenever the muscles were to be stimulated or not. A so-called on/off curve would provide a signal to determine when to stimulate.

Activation pattern for biceps femoris was made in Matlab, by finding the peak of contraction and include 3 samples before and 7 samples after (Figure 11.7).

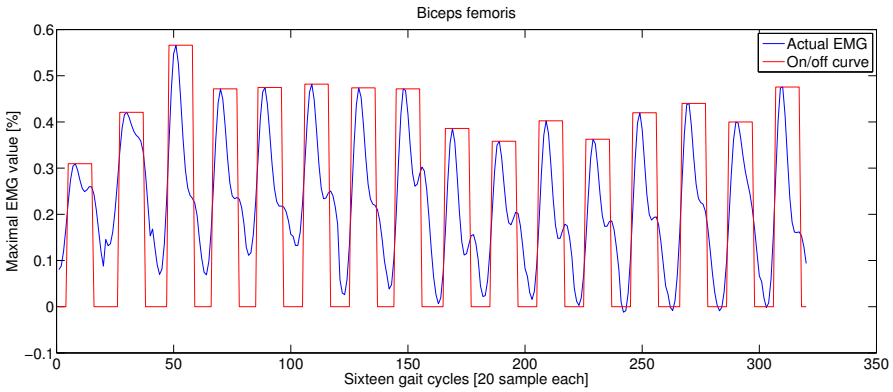

Figure 11.7: *The on/off curve found by the peak of contraction.*

Prediction of original EMG were then compared against the on/off curve (Table 11.6).

	on/off curve	**Original EMG**
Optimal configuration found	0.3993	0.7274

Table 11.6: *R^2 values obtained with optimal configuration found for input data, while testing original EMG compared with an on/off curve.*

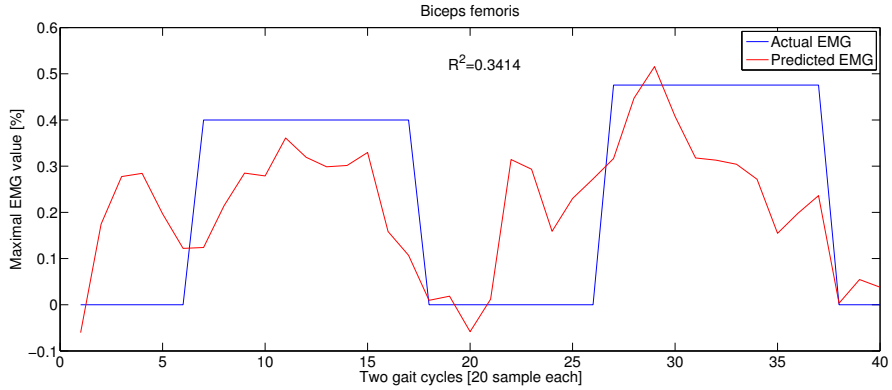

Figure 11.8: *Prediction of on/off curve for biceps femoris from the AB experimental data with 3 hidden layers, 40 neurons, bin-size of 5%, LM training algorithm and a moving average filter with 5 samples span.*

11.2 Summary of optimization

Initial configuration adapted from Wessberg et al. [2000] indicated a need for optimization in order to encounter prediction of EMG activity on the basis of IC signals. The evaluation of ANN parameters and input/output data revealed a room for improvements. Various parameters had been adjusted in order to find the best combination of settings to configure the ANN. Stepwise improvements of the model is shown in Table 11.7 with an initial $R^2 = 0.0975$ and final $R^2 = 0.7274$.

Steps of optimization	R^2
Initial configuration	0.0975
Increasing neurons to 40	0.1337
Increasing hidden layers to 3	0.1572
Using LM training algorithm	0.2237
Increasing bin-size to 5%	0.5774
Adding shift of 0%	0.5774
Smoothing signal with span of 5 samples	0.7274

Table 11.7: *Summary of optimization process.*

CHAPTER 12

Results

Optimized configuration of ANN and input/output data from rat 1 described in chapter 11 are applied to following cases:

- **Case 1:** Use 1 day of horizontal to test the model trained on the 3 days of horizontal.
- **Case 2:** Use 1 day of inclined to test the model trained on the 3 days of inclined.
- **Case 3:** Use 4 days of horizontal to test the model trained on 4 days of inclined.
- **Case 4:** Use 1 day of horizontal and inclined to test model trained on the 3 days of horizontal and inclined.

Case 1

Results from the AAN trained solely with data from 3 days of horizontal and tested with 1 day for biceps femoris (Figure 12.1) and vastus lateralis (Figure 12.2). A gross prediction of EMG for both muscles are noticeable but high fluctuations are represented during the shift between phases.

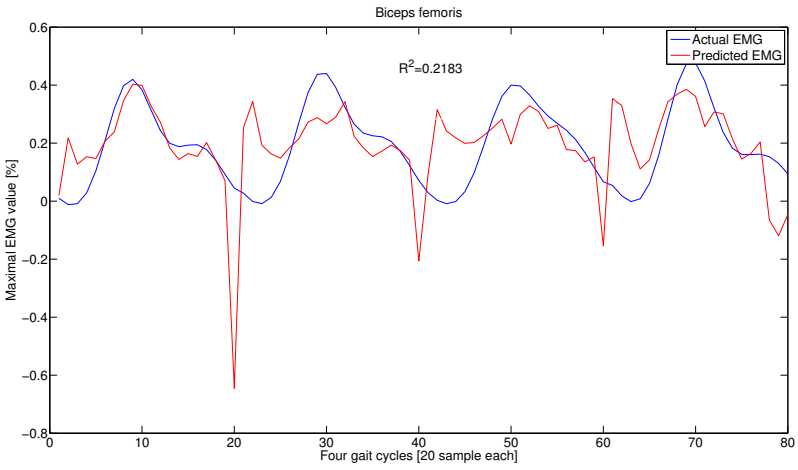

Figure 12.1: *Actual (blue) and predicted (red) EMG activity for biceps femoris, based on a data set consisting of horizontal treadmill walking.*

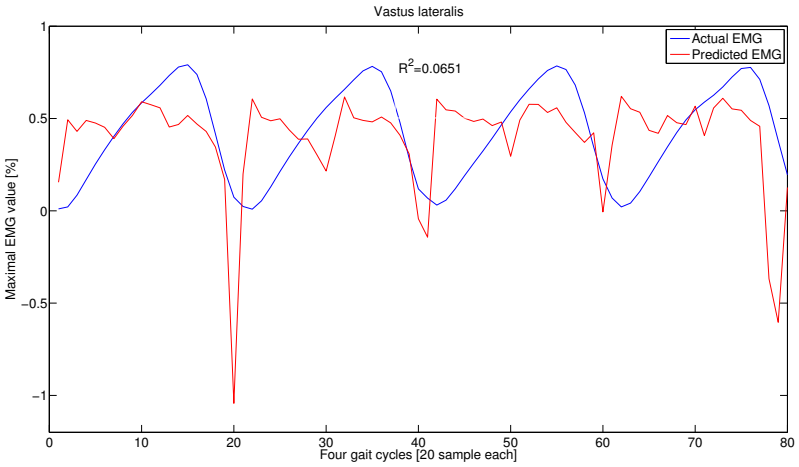

Figure 12.2: *Actual (blue) and predicted (red) EMG activity for vastus lateralis, based on a data set consisting of horizontal treadmill walking.*

Case 2

Results from the AAN trained solely with data from 3 days of inclined and tested with 1 day for biceps femoris (Figure 12.3) and vastus lateralis (Figure 12.4). A gross prediction of biceps femoris is noticeable but high fluctuations are represented during the muscles passive phase.

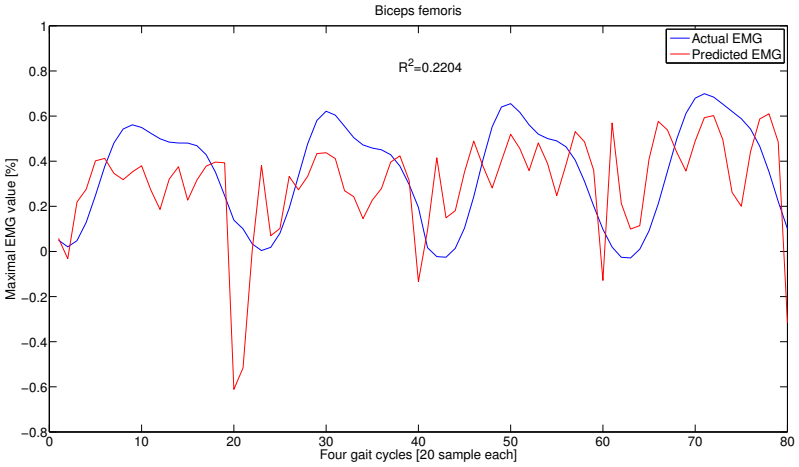

Figure 12.3: *Actual (blue) and predicted (red) EMG activity for biceps femoris, based on a data set consisting of treadmill walking with incline.*

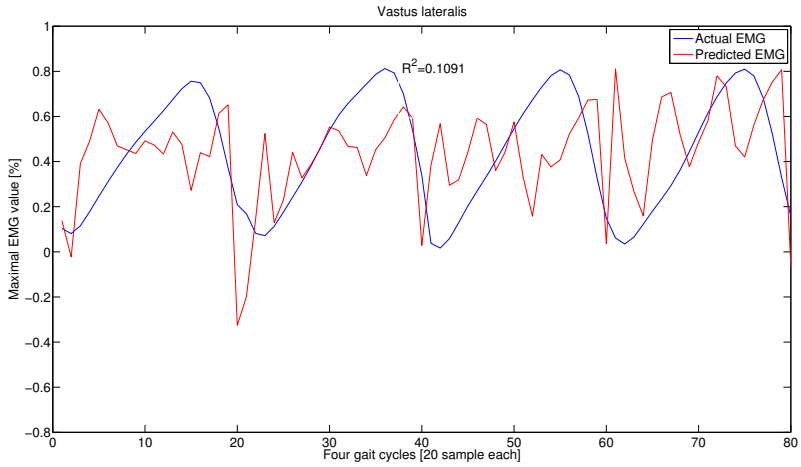

Figure 12.4: *Actual (blue) and predicted (red) EMG activity for vastus lateralis, based on a data set consisting of treadmill walking with incline.*

Case 3

Results from the AAN trained with data from 4 days of horizontal and tested with 4 days of inclined for rat 1 for biceps femoris (Figure 12.5) and vastus lateralis (Figure 12.6). Results from rat 2 trained on 2 days of horizontal and tested on 1 day of inclined for biceps femoris and vastus lateralis (Figure 12.7 and Figure 12.8).

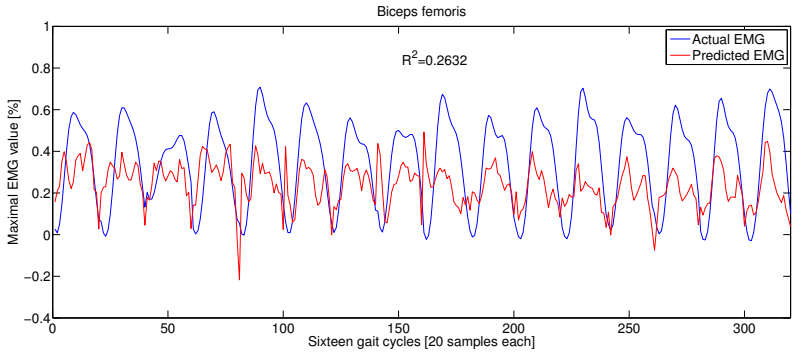

Figure 12.5: *Actual (blue) and predicted (red) EMG activity for biceps femoris in rat 1, based on a data set consisting of horizontal treadmill walking tested on inclined data.*

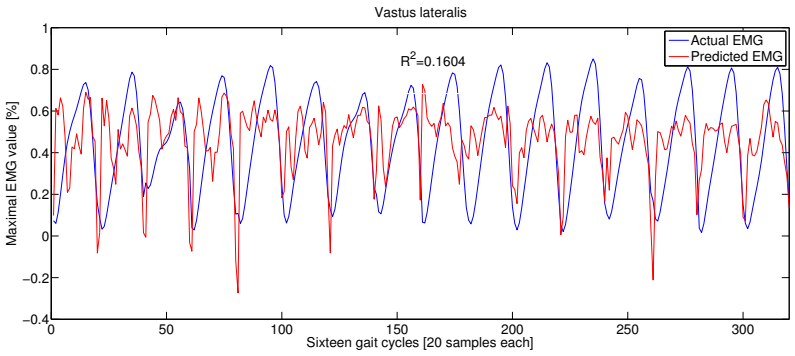

Figure 12.6: *Actual (blue) and predicted (red) EMG activity for vastus lateralis in rat 1, based on a data set consisting of horizontal treadmill walking tested on inclined data.*

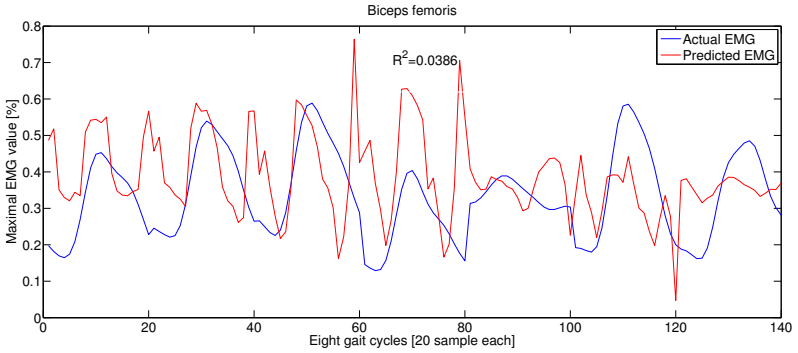

Figure 12.7: *Actual (blue) and predicted (red) EMG activity for biceps femoris in rat 2, based on a data set consisting of horizontal treadmill walking tested on inclined data.*

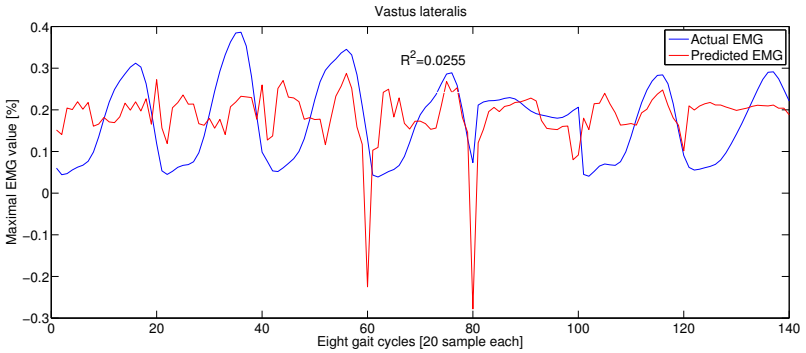

Figure 12.8: *Actual (blue) and predicted (red) EMG activity for vastus lateralis in rat 2, based on a data set consisting of horizontal treadmill walking tested on inclined data.*

Case 4

Results from the AAN trained with data from 3 days of horizontal and inclined and tested with 1 day of horizontal and inclined for rat 1 for biceps femoris (Figure 12.9) and vastus lateralis (Figure 12.10). Re-

sults from rat 2 trained on 10 sessions of horizontal and 5 sessions of inclined and tested on 2 sessions of horizontal and 2 sessions of inclined data for biceps femoris and vastus lateralis (Figure 12.11 and Figure 12.12).

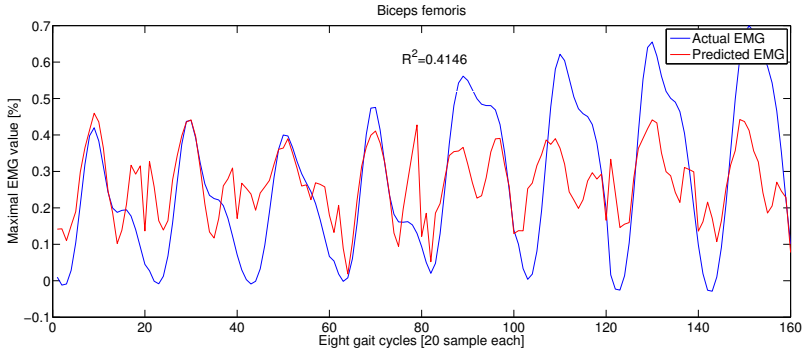

Figure 12.9: *Actual (blue) and predicted (red) EMG activity for biceps femoris in rat 1, based on a data set consisting of 3 full days of data and tested on 1 day of data.*

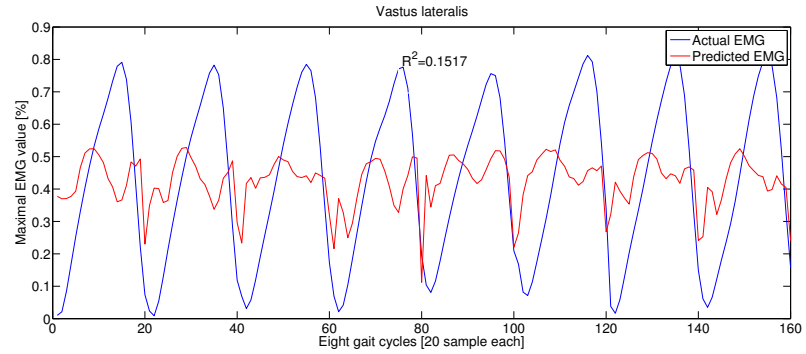

Figure 12.10: *Actual (blue) and predicted (red) EMG activity for vastus lateralis in rat 1, based on a data set consisting of 3 full days of data and tested on 1 day of data.*

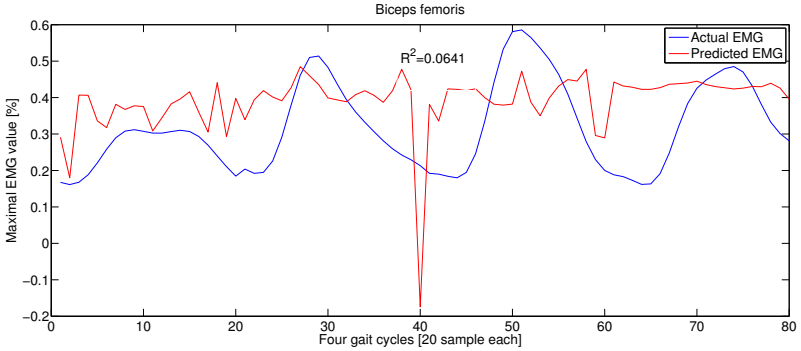

Figure 12.11: *Actual (blue) and predicted (red) EMG activity for biceps femoris in rat 2, based on a data set consisting of 15 sessions (10 horizontal/5 inclined) of data and tested on 4 sessions (2 horizontal/2 inclined) of data.*

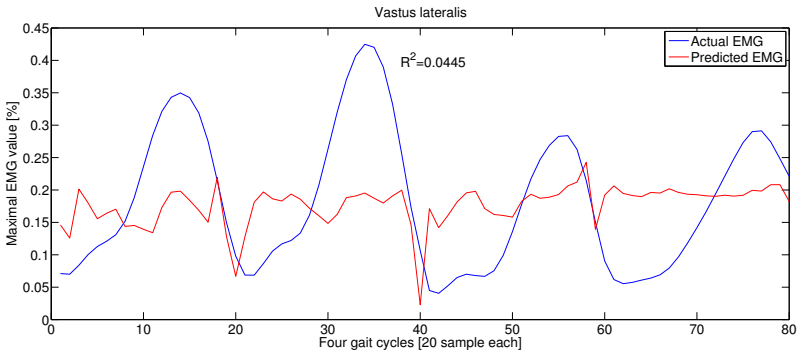

Figure 12.12: *Actual (blue) and predicted (red) EMG activity for vastus lateralis in rat 2, based on a data set consisting of 15 sessions (10 horizontal/5 inclined) of data and tested on 4 sessions (2 horizontal/2 inclined) of data.*

PART III

Synthesis

CHAPTER 13

Discussion

The ANN models created based on the experimental data were used to predict EMG patterns of locomotion from modulations in neural activity recorded in M1 of rats. Results of kinematics and modulation in neural activity during locomotion were expected due to similar findings in previous animal studies (Gillis and Biewener [2001]; Rossignol [1996]).

Though, limited knowledge and studies exist for evaluating restoration of locomotion by means of BMI applications (Fitzsimmons et al. [2009]; Song et al. [2009]), and therefore it was uncertain if neural activity from M1 in rats could be sufficient to predict EMG activity of target muscles. The findings of kinematics and visible modulation patterns of several PSTH's resemble previous findings to an extent, so we believe that research and focus could improve results in future BMI applications.

Improving prediction of the ANN

Performance of the ANN model rely on the inputs and outputs used for training. Quality of the inputs could be enhanced during several steps in the process: surgery, recordings and preparation of data.

The optimization process
In order to achieve prediction accuracies similar to those found by Wessberg et al. [2000], an optimization process of the ANN was performed. The chosen optimization approach gradually increased the prediction accuracy of the ANN. It is uncertain if the order and sequence of optimization steps had effect on the final predictions.

Surgery
The implanted electrode array in M1 gave a low amount of hindlimb responses from microstimulation, restricting the amount of hindlimb associated inputs and accuracy of the ANN. Leergaard et al. [2004] presented an adapted mapping of the rat brain on the basis of previous maps, with a fairly small hindlimb area. Individual anatomy of each rat could be a reason for variations and the depth of 1.7 mm should be adjusted accordingly. In a study predicting walking in monkeys by Fitzsimmons et al. [2009], neural activity from 60 neurons were needed for a sufficient prediction of constant walking which reveal the need of recording from more neurons.

Behavior of the rats was not monitored after surgery, where the rats might have bumped into edges of the cage and pushed the electrode further down or destroying neurons.

Recordings
Time stamps of IC spike activity were recorded using automatic thresholding. This threshold was set for each day of recording and therefore probably not the same. If the rat was not calm while setting the threshold, neural activity would force the threshold higher, oppressing information. One could avoid this by recording continuous data and manually do thresholding afterwards, leaving all information intact.

The used configuration of recording multi neurons could possibly decrease the characteristics of gait, due to the fact that a majority of channels were not associated with hindlimb activity. Microstimulations were performed before and after the experiment and showed different results. This give rise to uncertainty about the PSTH's and their reliability since the time of change is unknown. In addition, a low number of channels associated with hindlimb activity could have limited the performance of the ANN and oppress any clear modulation pattern in the neural activity.

Selection of speed for behavioral tasks can alter the gait cycle in rats, since stance phase decrease as result of increase in speed, whereas swing and stance in humans are stable around 40%/60%. Choosing a wrong speed could possible reduce the comparability between rats and humans.

A gait cycle duration ranging from 0.4 s to 0.7 s could be too much according to variations in length and ratio of swing and stand phase. Biceps femoris and vastus lateralis have shown to be active from the end of swing phase and throughout approximately 80 % of stance phase. This shift could have eliminated or reduced characteristics in the signals since signals are summed after normalization. Choice of speed have an unknown effect on fatigue and how it impact the characteristics of neural activity and EMG signal. Distinct changes might be unseen due to averaging signals.

Preparation of data
The total amount of data were recorded over five days but reduced due to exclusion of two rats and missing event detections. A larger amount of data with more days of recording and more rats would provide the ANN more information and cover a larger span of the input range.

Previous studies have stated an uncertainty in kinematics due to unstable markers because of skin movements. [Back and Clayton, 2000]

Skin movement could have affected the final outcome due to errors in digitizing markers and day to day variability in attaching the

markers. Especially the knee markers seemed to be influenced by skin movements, yielding a greater variation in knee angle. Suggestions by Fitzsimmons et al. [2009]; Gillis and Biewener [2001]; Thota et al. [2005] implied permanent ink or tattooing of the rats. Another approach to lower variability is to let the same experimenter apply markers.

A common process of preparing IC data is spike sorting. This option could have been applied if the recordings were continuously stored and reveal activity of single neurons. Spike sorting of the neural data could maybe indicate a more distinct pattern of activity during gait.

Performance of the ANN

The results from rat 1 generally showed a better prediction accuracy and a more distinctive prediction shape of the actual EMG signal for biceps femoris compared to vastus lateralis. This could maybe be explained by the fact that the optimization process of the ANN was based on biceps femoris.

The highest prediction accuracies were found in Case 4 for rat 1 with R^2 of 0.4146 for biceps femoris and Case 3 for rat 1 with R^2 of 0.1604 for vastus lateralis. Compared to Case 1 and 2 these better predictions are probably caused duo to the larger amount of data provided for the ANN in these cases. Wessberg et al. [2000] showed R^2 values ranging from 0.2025-0.6241 for muscle prediction using ANN which make the R^2 value from biceps femoris found in Case 4 for rat 1 acceptable.

Fast fluctuations are observed in most of the predictions, and could be caused by extrapolation occurring if the training model receive unknown test data, this could occur while training with horizontal waking and testing using data from inclined walking.

Case 1 and 2 were not calculated for rat 2 due to the low amount of sessions caused by missing event detections from IC recordings. The results from rat 2 in Case 3 and 4 showed low R^2 values compared to rat 1, which again probably are caused by the lower amount of data provided to the ANN. If the same amount of sessions were available for both rats it would have been possible to compare the prediction results between rats.

Scaling problems in Case 3 could yield an issue in regards to generalizing a prediction model, being unable to generalize between different tasks and environments. Day to day variability of IC recordings could change and was observed by results of microstimulation (Appendix E). [Song et al., 2009]

Similar findings were shown by Fitzsimmons et al. [2009] who compared backward trained models with forward walking and reverse.

Future prospects

Involving obstacles could probably invoke a clearer neural activity pattern, since M1 is main responsible for gait associated with visual demands. A clearer activity pattern could enhance the correlation between neural activity and muscle activity, resulting in a better prediction accuracy of the ANN.

Additional data for each rat could give a better generalized performance of the ANN. A larger amount of neural data could be obtained from each individual rat by implanting tetrodes. Using tetrodes would increase the number of recording sites and quantity of neural information. After establishing a robust ANN model with high quality inputs, further inclusion of additional muscles would allow complex movements to be carried out.

If a robust ANN is working well in offline mode, the next step would be to implement it in real-time BMI applications for restoring locomotion of SCI patients with FES.

CHAPTER 14

Conclusion

Spinal cord injury and related complications with reduced mobility have a great impact on quality of life. Restoration and aiding of gait control using BMI is still an unexplored and unevaluated area with only few studies and knowledge about possibilities.

An experiment has been conduced during the project period, in order to obtain neural data from M1 and EMG signals from biceps femoris and vastus lateralis in healthy rats for use in an ANN. An optimization process of the ANN was performed by trying different configurations and parameters of the ANN together with optimization of the data provided. Through this optimization process the performance accuracy of R^2 was increased from 0.0975 to 0.7274.

The predictions from Case 1 and Case 2 did not follow the activation pattern of the actual EMG pattern and had corresponding low prediction accuracies. Case 3 showed amplitude scale problems compared with actual EMG, but demonstrated visible activation patterns with R^2 = 0.2632 and R^2 = 0.1604 for biceps femoris and vastus lateralis from rat 1, respectively. The results from rat 1 in Case 4 showed better prediction results, and especially the prediction of biceps femoris showed a high accuracy of R^2 = 0.4146 which lies within the range of the R^2 = 0.2025-0.6241 found by [Wessberg et al., 2000]. The predictions accuracies from rat 2 in Case 3 and 4 were low due to the limited amount of data provided to the ANN. The best prediction results were achieved with data from 4 days used for training, indicatings that more data are needed in order to secure good predictions.

Further advancement and usage of prediction for FES control signals need further attention and evaluation, since predictions are rough and possess suddenly fluctuations. Muscle contractions should be gradually and smooth, without sudden fluctuations as seen in the results. Predictions did a better job defining beginning and end of the muscle activation, which with improvements could be used for predicting when and when not to stimulate with FES. Possibilities of ANN optimization and fine tuning were demonstrated and implied individual adjustments are necessary for individual data sets and BMI applications.

Evaluating an ANN as a decoding model in pursuing restoration of gait, for instance by interaction with BMI applications, showed po-

tential results and, by a refinement could lead to better predictions and bring restoration of gait one step closer to realization

Bibliography

Anderson, K. D. (2004). Targeting recovery: Priorities of the spinal cord-injured population. *Journal of Neurotrauma*, 21(10):1371–1383.

Back, W. and Clayton, H. M. (2000). *Equine Locomotion*. Saunders (W.B.) Co Ltd.

Basler (2010). *Basler A600f - User manual*. Basler AG, An der Strusbek 60 - 62, 22926 Ahrensburg, Germany, v. 9 edition.

Bauman, M. J., Wagenaar, J. B., Gaunt, R. A., and Weber, D. J. (2011). Online feedback control of functional electrical stimulation using dorsal root ganglia recordings. *IEEE*.

Beale, M. H., Hagan, M. T., and Demuth, H. B. (2012). *Neural Network Toolbox™ User's Guide R2012a*. MathWorks, The MathWorks, Inc. 3 Apple Hill Drive Natick, MA 01760-2098.

Beloozerova, I. N., Sirota, M. G., and Swadlow, H. A. (2003). Activity of different classes of neurons of the motor cortex during locomotion. *The Journal of Neuroscience*, pages 1087–1097.

Bronzino, J. D. (1999). *The Biomedical Engineering Handbook*. CRC Press, second edition edition.

Byrne, J. H. and Dafny, N. (2000). *Neuroscience Online Book*. Department of Neurobiology and Anatomy at The University of Texas Medical School at Houston.

Cenci, A. M., Whishaw, I. Q., and Schallert, T. (2002). Animal models of neurological deficits: how relevant is the rat? *Nature Neuroscience*, 3:574–579.

Chapin, J. K., Moxon, K. A., Markowitz, R. S., and Nicolelis, Miguel A. L, . (1999). Real-time control of a robot arm using stimultaneously recorded neurons in the motor cortex. *Nature Neuroscience*.

Donaldson, N., Rushton, D., and Tromans, T. (1997). Neuroprostheses for leg function after spinal-cord injury. *The Lancet*, 350:711.

Drew, T. (1988). Motor cortical cell discharge during voluntary gait modification. *Brain Research*.

Ethier, C., Oby, E. R., Bauman, M. J., and Miller, L. E. (2012). Restoration of grasp following paralysis through brain-controlled stimulation of muscles.

Everett, T. and Kell, C. (2010). *Human Movement An Introductory Text*. Elsevier, 6th edition edition.

Fagg, A. H., Hatsopoulos, N. G., Lafuente, V., Moxon, K. A., Nemati, S., Rebesco, J. M., Romo, R., Solla, S. A., Reimer, J., Tkach, D., Pohlmeyer, E. A., and Miller, L. E. (2007). Biomimetic brain machine interfaces for the control of movement. *The Journal of Neuroscience*.

Fitzsimmons, N. A., Lebedev, M. A., Peikon, I. D., and Nicolelis, M. A. L. (2009). Extracting kinematic parameters for monkey bipedal walking from cortical neuronal ensemble activity. *Frontiers in Integrative Neuroscience*.

Gill, T. J., Smith, G. J., Wissler, R. W., and Kunz, H. W. (1989). The rat as an experimental animal. *Science/AAAS*, 245(4915):269–276.

Gillis, G. B. and Biewener, A. A. (2001). Hindlimb muscle function in relation to speed and gait: in vivo patterns of strain and activation in a hip and knee extensor of the rat (rattus norvegicus). *Journal of Experimental Biology*, 204(15):2717–31.

Hagan, M. T., Demuth, H. B., and Beale, M. (1996). *Neural Network Design*. PWS Publishing.

Hochberg, L. R., Serruya, M. D., Friehs, G. M., Mukand, J. A., Saleh, M., Caplan, A. H., Branner, A., Chen, D., Penn, R. D., and Donoghue, J. P. (2006). Neuronal ensemble control of prosthetic devices by a human with tetraplegia. *Nature*.

Jensen, W., Rousche, P. J., and Chiganos, T. C. (2006). A method for monitoring intra-cortical motor cortex responses in an animal model of ischemic stroke. *EMBS Annual International Conference*.

João, F., Amado, S., Armada, P., Maurício, A. C., and Veloso, A. (2010). Segmental kinematic analysis using a tridimensional reconstruction of rat hindlimb: Comparison between 2d and 3d joint angles.

Johnston, T. E., Betz, R. R., Smith, B. T., Benda, B. J., Mulcahey, M. J., Davis, R., Houdayer, T. P., Pontari, M. A., Barriskill, A., and Creasey, G. H. (2005). Implantable fes system for upright mobility and bladder and bowel function for individuals with spinal cord injury. *Spinal Cord*, 43(12):713–23.

Kandel, E., Schwartz, J., and Jessel, T. (2000). *Principles of neural science*. McGraw-Hill.

Keith, M. W., Peckham, H., Thrope, G. B., Stroh, K. C., Smith, B., Buckett, J. R., Kilgore, K. L., and Jatich, J. W. (1989). Implantable functional neuromuscular stimulation in the tetraplegic hand. *The Journal of Hand Surgery*, 14(3):524–530.

Latash, M. L. (1998). *Neurophysiological Basis of Movement*. Human Kinetics.

Leblond, H., L'Espérance, M., Orsal, D., and Rossignol, S. (2003). Treadmill locomotion in the intact and spinal mouse. *The Journal of Neuroscience*, pages 11411–11419.

Leergaard, T. B., Alloway, K. D., Pham, T. A. T., Bolstad, I., Hoffer, Z. S., Pettersen, C., and Bjaalie, J. G. (2004). Three-dimensional topography of corticopontine projections from rat sensorimotor cortex: Comparisons with corticostriatal projections reveal diverse integrative organization. *The journal of comparative neurology*, pages 306–322.

Liverman, C. T., Altevogt, B. M., and Joy, J. E. (2005). *Spinal Cord Injury : Progress, Promise, and Priorities*. National Academies Press.

Martini, F. H. (2006). *Fundamentals of Anatomy and Physiology*. Pearson, 7th edition edition.

McDonald, J. W. and Sadowsky, C. (2002). Spinal-cord injury. *The Lancet*, 359:417–425.

Michael-Titus, A., Revest, P., and Shortland, P. (2010). *The Nervous System - Basic science and clinical conditions*. Elsevier.

Neafsey, E. J., Bold, E. L., Haas, G., Hurley-Gius, K. M., Quirk, G., Sievert, C. F., and Terreberry, R. R. (1986). The organization of the rat motor cortex: A microstimulation mapping study. *Brain Research Reviews*.

NSCISC (2011). Spinal cord injury facts and figures at a glance. Technical report, National Spinal Cord Injury Statistical Center, Birmingham, Alabama.

Nudo, R. J. (2007). Postinfarct cortical plasticity and behavioral recovery. *Journal of American Heart Association*.

Oby, E. R., Ethier, C., Bauman, M. J., Perreault, E. J., Ko, J. H., and Miller, L. E. (2010). *Statistical Signal Processing for Neuroscience and Neurotechnology*, chapter 11. Elsevier.

Pearson, K. G., Acharya, H., and Fouad, K. (2005). A new electrode configuration for recording electromyographic activity in behaving mice. *Journal of neuroscience methods*, pages 36–42.

Peckham, H. P. and Knutson, J. S. (2005). Functional electrical stimulation for neuromuscular applications.

Pereira, J. E., Cabrita, A. M., Filipe, V. M., Bulas-Cruz, J., Couto, P. A., Melo-Pinto, P., Costa, L. M., Geuna, S., Maurício, A. C., and Varejao, A. S. P. (2006). A comparison analysis of hindlimb kinematics during overground and treadmill locomotion in rats. *Behavioural Brain Research*, pages 212–218.

Pohlmeyer, E. A., Oby, E. R., Perreault, E. J., Solla, S. A., Kilgore, K. L., Kirsch, R. F., and Miller, L. E. (2009). Toward the restoration of hand use to a paralyzed monkey: Brain-controlled functional electrical stimulation of forearm muscles. *PLoS ONE*.

Popovic, D. B. and Sinkjær, T. (2003). *Control of movement for the physically disabled*. Center for Sensory-Motor Interaction, Department of Health Science and Technology.

Popovic, M. R., Popovic, D. B., and Keller, T. (2002). Neuroprostheses for grasping. *Neurological Research*, 24:443–452.

Purves, D., Augustine, G. J., Fitzpatrick, D., Hall, W. C., LaMantia, A.-S., McNamara, J. O., and Williams, S. M. (2004). *Neuroscience*. Sinauer Associates, Inc., 3rd edition edition.

Rossignol, S. (1996). *Neural control of stereotypic limb movements*, chapter 12. Handbook of Physiology. Oxford University Press.

Roy, R. R., Hutchison, D. L., Pierotti, D. J., Hodgson, J. A., and Edgerton, V. R. (1991). Emg patterns of rat ankle extensors and flexors during treadmill locomotion and swimming. *Journal of App. Physiol.*, pages 2522–2529.

Sanchez, J. C. and Principe, J. C. (2007). *Brain-Machine Interface Engineering*. Morgan & Claypool.

Slutzky, M. W., Jordan, L. R., Lindberg, E. W., Lindsay, K. E., and Miller, L. E. (2011). Decoding the rat forelimb movement direction from epidural and intracortical field potentials. *J Neural Eng*, 8(3).

Song, W., Ramakrishnan, A., Udoekwere, U. I., and Giszter, S. F. (2009). Multiple types of movement-related information encoded in hindlimb/trunk cortex in rats and potentially available for brain-machine interface controls. *IEEE Transactions on Biomedical Engineering*.

Tate, D. G., Boninger, M. L., and Jackson, A. B. (2011). Future directions for spinal cord injury research: recent developments and model systems contributions. *Arch Phys Med Rehabil*, 92(3):509–15.

TDT (2011). *TDT System 3 Manual*. Tucker-Davis Technologies, 11930 Research Circle Alachua, FL 32615, USA.

Thota, A. K., Watson, S. C., Knapp, E., Thompson, B., and Jung, R. (2005). Neuromechanical control of locomotion in the rat. *Journal of Neurotrauma*, 22(4):442–465.

Tu, J. V. (1996). Advantages and disadvantages of using artificial neural networks versus logistic regression for predicting medical outcomes. *Journal of Clinical Epidemiology*, 49(11):1225–1231.

Vaughan, C. L., Davis, B. L., and O'Connor, J. C. (1999). *Dynamics of Human Gait*. Kiboho Publishers.

Webster, J. G. (2006). *Encyclopedia of Medical Devices and Instrumentation*. John Wiley Publisher.

Wessberg, J., Stambaugh, C. R., Kralik, J. D., Beck, P. D., Laubach, M., Chapin, J. K., Kim, J., Biggs, J. S., Srinivasan, M. A., and Nicolelis, M. A. L. (2000). Real-time prediction of hand trajectory by ensembles of cortical neurons in primates. *Nature*.

Wolpaw, J. R., Birbaumer, N., McFarland, D. J., Pfurtscheller, G., and Vaughan, T. M. (2002). Brain-computer interfaces for communication and control. *Clinical Neurophysiology*.

Appendices

APPENDIX A

Northwestern University, Chicago

The 3rd semester of the master education in medical systems took place as graduate students at Northwestern University (NWU), Chicago, as interns in the Miller Lab (the Miller laboratory of Limb Motor Control). Additional, in cooperation with the lab of Matthew Tresch, other graduate students and Rehabilitation Institute of Chicago (RIC).

We took part in the start-up phase of a project evaluating a strategy for restoring motor function following paralysis, together with a lab colleague. Experiments were conducted on rats, with the long term prospectives of increasing quality of life for spinal cord injured patients, by simplifying control of limb movements by using functional electrical stimulation.

The intended goal was to return to Denmark with pilot data and further work planned for easy transition from 3rd to 4th semester. Although this was not the case due to complications, we returned with practical experience, knowledge and experimental ideas. This outcome forced us to start from scratch, with a new experiment based on ideas.

A.1 Practical experience

Being a part of the new project implied experimental work and rat surgeries. Before any experiments we attended a course with theoretical and practical exercises dealing with handling, care and euthanasia of rats, mice and non-human primates. A few acute and chronic surgeries were seen with procedures for sterile surgery, implanting intracortical (IC) electrodes, stimulation and recordings from single wire electrodes, monitoring of vital signs and recovery, before these task where performed several times without supervision.

A Tucker-Davies Technologies (TDT) system was set up for recordings and controllable artificial neural activity were used to test the system. Neural activity from implanted rats were recorded while walking around in their cages, and later on while running on a treadmill.

Furthermore, we observed dissection of the rat hindlimb and implantation of EMG electrodes in several muscles. EMG signals were tested while the rat walked on a treadmill with markers, which were captured by a VICON motion capture system.

A.2 Complications

We did not return with the desired data as expected due to complications. Complications in the surgery or recovery phase resulted in euthanasia of rats and postponing of system test with the TDT and VICON recording. EMG implantation on a rat went well and good signals were recorded while walking on a treadmill. Unfortunately, the rat teared out the connecter attached to the back a few days after initial EMG recordings.

A.3 Additional experience

Additional experience were gained during the stay at NWU. Several non-human primate experiments focussing on hand grasp were observed and assistance provided by means of regulating anesthesia, inserting electrodes and noting down progress during the experiments. Furthermore, we took part of a 24 hours terminal non-human primate experiment assisting monitoring of vital signs etc.

By observing and visiting other laboratories at NWU we obtained insight in other areas of neuroscience experiments.

Experience of manufacturing tetrodes was obtained by learning from a graduate student, who used these refined electrode for recording. The advantage of tetrodes is the four-site recording possibilities and adjustment of insertion depth in the brain. Further distinction and spike sorting becomes easier and adjustment of depth can encounter possible cell death.

General knowledge about current research in rehabilitation and neuroscience were obtained through talks and presentations at RIC and attendance at the annual Society for Neuroscience conference.

A.4 Summary

Due to complications with animal experiments and recordings during our stay, we did not accomplish final recordings with combined IC signals from primary motor cortex, EMG from hindlimb muscles and VICON data, while running on a treadmill.

Although we did not return with pilot data for immediately processing and analysis on our 4th semester, we gained valuable experimental ideas and experience which have been beneficial for making new experiments. Familiarity with the TDT system, handling and experiments with animals, surgery procedures for implanting electrodes

and motion capture recordings have been valuable knowledge for 4th semester.

APPENDIX B

Artificial Neural Network

An artificial neural network (ANN) requires no physical insight of the system investigated and is therefore suitable for many applications. The ANN is robust, easy to implement and are able to find accurate approximations relations between input and output which can be used for prediction. [Sanchez and Principe, 2007]

The ANN is organized in simple elements, which can be connected to expand computational performance. Neurons are the base elements of a network (Figure B.1) and consists of inputs, weights and a transfer function. [Beale et al., 2012] The input P can either be recorded

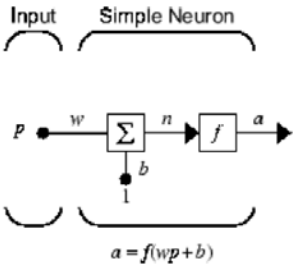

Figure B.1: *Set up of a simple neuron. [Beale et al., 2012]*

signals or be signals from other neurons, which is sent into the neuron where weights are multiplied with the input P. A constant bias weight is added before sending the net input into a transfer function. The transfer function can have various forms and the most common ones are linear, log-sigmoid or tan-sigmoid. [Beale et al., 2012]

Standard configuration of ANN is a two layer network consisting of 10 neurons which is powerful. But if the result is not sufficient, increasing the number of neurons and hidden layers containing nonlinear function improve (multilayer network - Figure B.2) the flexibility of the network and allow the network to encounter complex nonlinear relationships. [Beale et al., 2012]

but by increasing the amount of neurons more computation time is needed and overfitting has to be taken into account. [Beale et al., 2012]

Training, validation and test

Training of the network is necessary after ended configuration. To ensure good performance of the model it is important to cover as

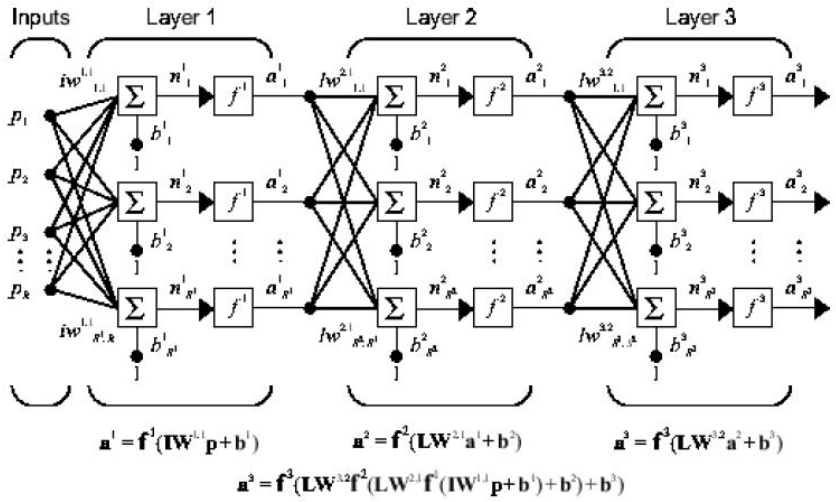

Figure B.2: *Structure of a three layered ANN model [Beale et al., 2012]*

much of the expected input-range in the training data, since ANNs are not good at extrapolating. Normalization of input- and output data are often carried out to improve performance of training. [Beale et al., 2012]

Input data are divided into two different groups in order to evaluate and train the network. A training group is used to update the weights and bias. The validation group is comparing the performance by mean square error and detection of over fitting and a test group with unused data. The ANN is created from the best performing network and belonging weights and bias chosen upon the lowest error from validation, and is ready to be taken into use and tested on new data. [Beale et al., 2012]

Different training functions can be used for the ANN and varies in computation speed, memory usage and efficiency depending on size of data sets. Choosing a single training function can therefore be difficult and must be chosen from the complexity of the problem and according to desired goal (optimal speed, memory usage or efficiency). [Beale et al., 2012]

Backpropagation is an often used training method. The method use the inputs and targets until a function can be approximated for predicting the output vectors from the input vectors. First, the training method compute the propagation and the error signal of the system. The error signal is multiplied with the weights of the network backwards in the system and finally the output of the network is computed forwards again. A well trained backpropagation network is able to generalize and produce a good output result when provided with unknown test data. [Beale et al., 2012; Hagan et al., 1996]

APPENDIX C

Intracortical electrode manufacturing

This appendix describes the process of manufacturing a 4x4 (16) intracortical electrode array for implantation in motor cortex of the rats for assessment of intracortical signals.

List of materials

- 2 x board-to-board-connector with 2x4 rows, 2mm pitch and dimensions of (4.4 mm x 8 mm x 4 mm) (Harwin M22-7140442)
- Teflon Insulated tungsten wire (100 μm in coated diameter, 50 μm in bare diameter), length of 50 mm
- Custom made mold with 4x4 holes of 2/3 mm in between.
- Dental acrylic (Heraeus Kulzer Paladur)
- Superglue
- Microscope
- Tweezer
- Wooden sticks
- Soldering iron and tin solder
- Candle and lighter
- 4 pin male-to-male array
- 16 x crocodile clamps
- Acupuncture needle
- Tape
- Scissor
- Paper towel with distilled water
- Scalpel
- Frame/stand
- Yellow paper and graph paper
- Voltmeter

Step 1 - Preparation of workspace

A yellow piece of paper is fixated above a graph paper on the workspace table. The Yellow paper is used as background for storing electrode wires and easy visibility. The microscope is adjusted and focused for proper handling. (Figure C.1)

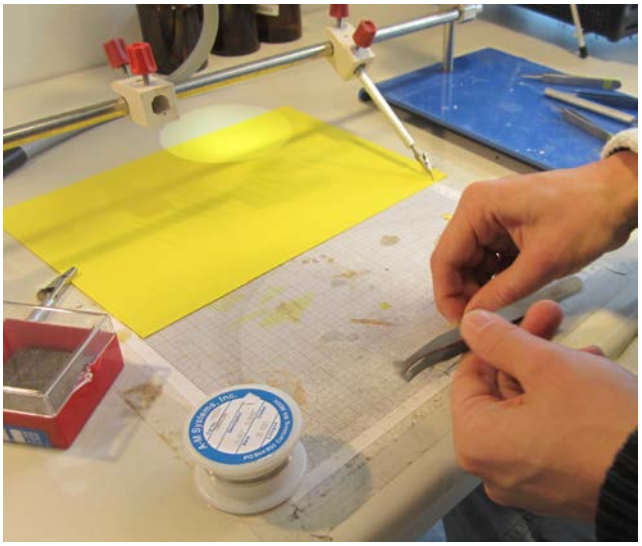

Figure C.1: *The workspace with a fixated piece of yellow paper and graph paper.*

Step 2 - Preparation of wires

The tungsten wire is handled with a tweezer and cut into 16 pieces, with a length of 5 cm each, measured on the graph paper. The candle is lit and used to remove insulation in the end of the wires. Paper towels with distilled water are used to remove possible dirt and improve contact.

Step 3 - Attaching wires to connector

A board-to-board-connector is fixated in the frame and wires are attached by soldering to the pins. Each wire is firmly stretched after attachment to check robustness. Connection between uninsulated wire and connecter is tested with a voltmeter when all wires are attached to the connector. A 4 pin male-to-male array is inserted in the board-to-board-connector to make testing easy. The uninsulated ends are cut off after testing and step 3 is repeated for the other board-to-board-connector and the two connecters are put together with superglue. (Figure C.1)

Step 4 - Attaching wires to connector

The mold for arranging the wires are fixated in the stand together with the connector. A piece of tape is put over the holes in the mold and pierced with a puncture needle, preventing the dental acrylic to stick to the mold later. Each wire is put into corresponding holes in the mold with a tweezer to form the 4x4 shape and a crocodile clamp is attached in the end to straighten and make tension. This procedure can be done with/without use of a microscope. (Figure C.2)

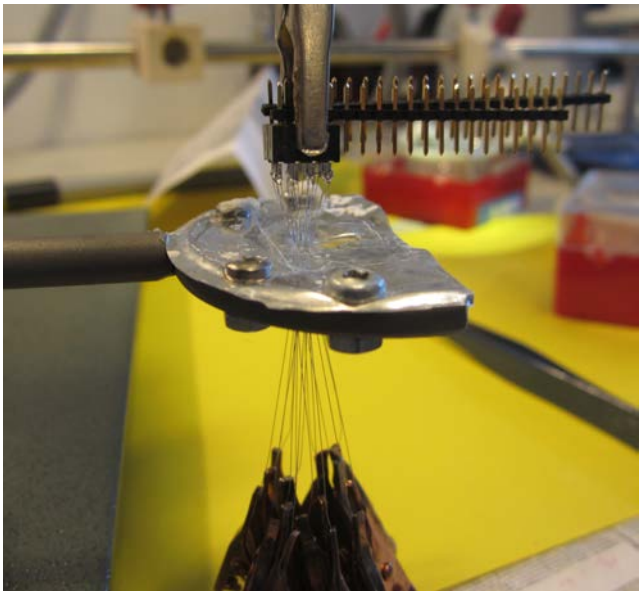

Figure C.2: *The wires are guided through the holes in the mould and a clamp attached to the end to hold the wires in place.*

Step 5 - Applying dental acrylic base

Dental acrylic is mixed under a fume hood to a desired consistence and applied to the electrode wires and connector until fully covered. Wooden sticks are attached to the side of the connector before cutting the wires. Unnecessary acrylic is removed with a scalpel. The finished IC electrode array is sent to be laser cut. (Figure C.3)

Figure C.3: *Applying dental acrylic in layers to cover the wires and adding wooden sticks before laser-cutting.*

APPENDIX D

EMG electrode design and manufacturing

This appendix describes the process of manufacturing a bipolar EMG electrode for implantation in biceps femoris and vastus lateralis of the rats for assessment of EMG signals.

List of materials

- Multi-stranded Teflon coated annealed stainless steel wire (A-M systems, Catalog Number 793200) Bare diameter: 0.0762 mm, coated diameter: 0.14 mm
- Cooner wire AS631, coated diameter 0.26 mm
- Board-to-board-connector with 2x4 rows, 2mm pitch and dimensions of (4.4 mm x 8 mm x 4 mm) (Harwin M22-7140442)
- Microscope
- Ruler
- Scissor
- Frame/stand
- Soldering iron and special solder for stainless steel
- Dental acrylic (Heraeus Kulzer Paladur)
- Voltmeter
- Needle

Step 1 - Preparation of workspace

A yellow piece of paper is fixated above a graph paper on the workspace table. The Yellow paper is used as background for storing electrode wires and easy visibility. The microscope is adjusted and focused for proper handling.

Step 2 - Preparation of wires

The electrode exists of two multi-stranded wires each with a length of 68 cm. On each wire two left-handed overhand knots and a right-handed overhand knot are made on top of each other 28 cm from the ends of the wires (Figure D.1). A de-isolation of 2 mm are made with a scalpel 1 mm and 5 mm after the knots on the remaining part of 6 cm under a microscope. Two pieces of ground wire (5 cm and 10 cm) are cut off and de-isolated in both ends.

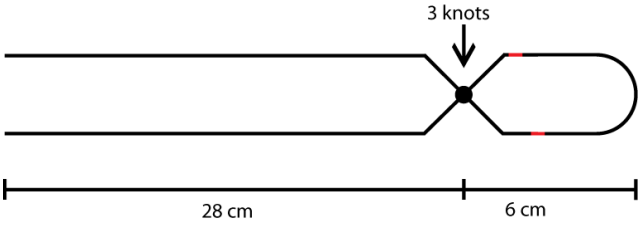

Figure D.1: *A figure of the EMG electrode which show the dimensions and the de-isolated parts of the electrode which are marked with red color.*

Step 3 - Soldering

The multi-stranded wire and ground wires are soldered to a board-to-board-connector and the connection tested with a voltmeter. When connection is ensured, dental acrylic is applied to the socket to secure from physical stress.

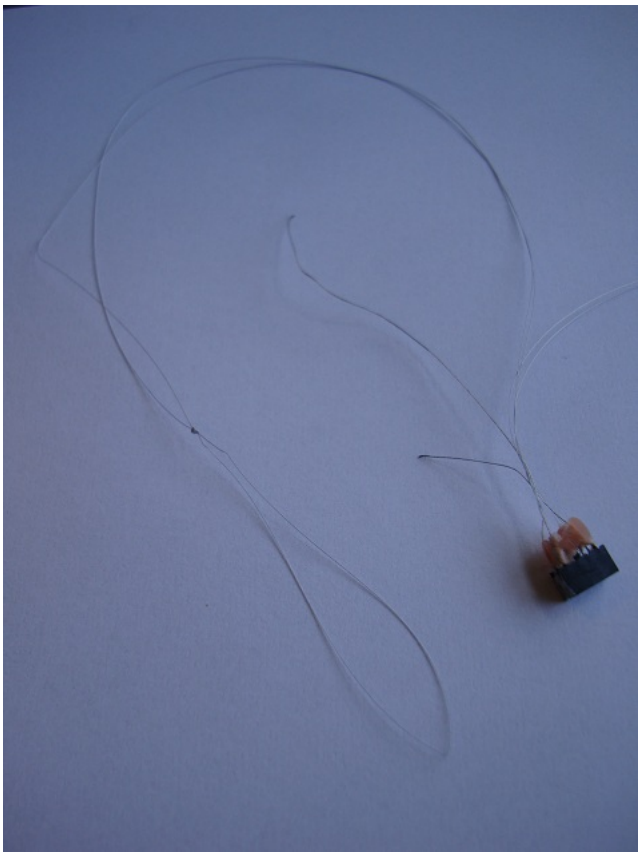

Figure D.2: *The picture show a manufactured EMG electrode ready to be implemented.*

APPENDIX E

Results from microstimulation

Microstimulation was done twice for each rat during the time of experiment. First stimulation was made a few days after surgery, allowing the rat to recover, and a second stimulation after ended experiments to see possible changes and causes of changed signals.

Responses of the micro stimulation were divided into categories of hindlimb response, other response and no response.

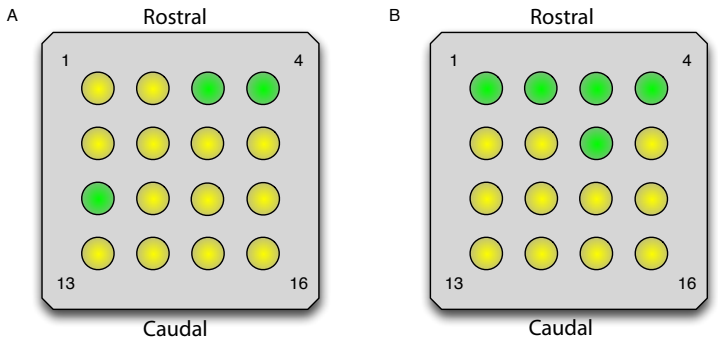

Figure E.1: *Rat 1: Responses from microstimulation on day 1 (A) and day 2 (B). Green represents responses in hindlimb area, Yellow other responses and Red no response.*

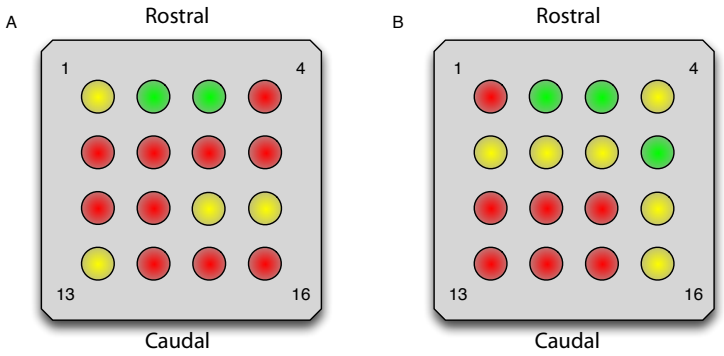

Figure E.2: *Rat 2: Responses from microstimulation on day 1 (A) and day 2 (B). Green represents responses in hindlimb area, Yellow other responses and Red no response.*